Fluid Phase Equilibria 299 (2010) 1–23

Contents lists available at ScienceDirect

Fluid Phase Equilibria

journal homepage: www.elsevier.com/locate/fluid

A duality-based optimisation approach for the reliable solution of (*P*, *T*) phase equilibrium in volume-composition space

Frances E. Pereira, George Jackson, Amparo Galindo, Claire S. Adjiman*

Department of Chemical Engineering, Centre for Process Systems Engineering, Imperial College London, South Kensington Campus, London SW7 2AZ, United Kingdom

ARTICLE INFO

Article history:
Received 15 March 2010
Received in revised form 5 August 2010
Accepted 6 August 2010
Available online 14 August 2010

Keywords:
Phase equilibrium
Phase stability
Helmholtz free energy
Global optimisation
Equations of state
Augmented van der Waals equation
Statistical associating fluid theory (SAFT)

ABSTRACT

A reliable algorithm for the solution of fluid phase equilibrium at constant pressure and temperature (*P*, *T* flash) is presented. The approach is applicable to multi-component mixtures described with general equations of state and is based on a formulation of *P*, *T* phase equilibrium as a dual optimisation problem in volume-composition space, translated away from the Gibbs free energy to the Helmholtz free energy. This formulation facilitates the use of guaranteed solution algorithms, particularly in the case of sophisticated equations of state (EOSs) such as SAFT (statistical associating fluid theory), because such representations are higher-than-cubic functions in volume and are formulated in the Helmholtz free energy. With the proposed algorithm (which is based on a combination of local and global optimisation, where the number of subproblems to be solved globally is kept at a minimum) one is guaranteed to identify the number of stable phases present at equilibrium, along with their properties, without any need for initial guesses, or indeed any *a priori* knowledge about the behaviour of the system. The method is applicable to the calculation of any kind of fluid phase behaviour (e.g., vapour–liquid (VLE), liquid–liquid (LLE), vapour–liquid–liquid (VLLE), etc.). Several algorithmic options are investigated and their computational performance compared. A prototype implementation is used to determine the fluid phase equilibria of a number of binary and ternary systems, where the thermodynamic properties are calculated through a molecular-based EOS. Examples are shown for the VLE and VLLE for mixtures modelled with an augmented van der Waals EOS, a non-cubic EOS that incorporates the Carnahan and Starling representation of the repulsive interactions. Further examples are presented for VLE and VLLE in polymer systems, modelled with an EOS of the generic SAFT form. Fluid phase equilibrium calculations for polymer systems are notoriously difficult, and convergence problems are often encountered, even with good initial guesses. The proposed method is found to be reliable in all cases examined.

1. Introduction

The reliable determination of phase equilibrium is important in process and product design, as the appearance and disappearance of phases, and the composition of the stable phases, greatly affect process performance and product end-use properties. The phases at equilibrium depend on key design variables such as total composition, temperature and pressure. Within process modelling, the solution of phase equilibrium is the task to which the majority of CPU time is devoted. Even for binary mixtures, this problem can be challenging [1–3], due to the high degree of nonlinearity and the presence of discontinuities.

In many applications, the phase equilibrium problem at given pressure, temperature and total composition, the *P*–*T* flash, is of interest. This problem can be briefly described as follows: Given a multi-component mixture with specified total composition, pressure and temperature, how many stable equilibrium phases are present and what are their properties? The solution of phase equilibrium lies at the global minimum of the system's total Gibbs free energy [4]. This function is related to the intensive Gibbs free energy which has the natural variables $\underline{x}$, *P*, *T*, where $\underline{x}$ is a vector of component mole fractions, *P* is pressure and *T* is temperature. One particularly challenging aspect of the formulation is that the number of phases is generally unknown [5].

There is a large body of work on this subject, the most successful general concept to date being the alternating stability test/flash approach first introduced by Michelsen [6–8]. The development of reliable methods for the solution of phase equilibrium and stability remains an active area of research. A number of deterministic techniques have been proposed, in which analysis of or insight into the problem is used to increase the likelihood of finding the stable solution (e.g., [9–15]). A global analysis of the solution space is undertaken in several of these algorithms, e.g., ([11,15]), but without a formal guarantee of convergence. Such approaches are

* Corresponding author. Tel.: +44 20 7594 6638; fax: +44 20 7594 6606.
E-mail address: c.adjiman@imperial.ac.uk (C.S. Adjiman).

0378-3812/$ – see front matter © 2010 Elsevier B.V. All rights reserved.
doi:10.1016/j.fluid.2010.08.001

particularly valuable where computational speed is a prime consideration. The correct solution is identified in many cases, but not in some difficult instances as discussed in [16–20]. Several *guaranteed* deterministic techniques have also been developed, such as those discussed in [21–27], where the focus is placed on providing a mathematical guarantee of finite convergence to within a tolerance ϵ of the solution. Through the use of interval analysis, it is possible to extend the guarantee of correctness so that mathematical and computational convergence can be ensured, regardless of the round-off error, as shown in [18,28–31]. Finally, a number of stochastic algorithms have been developed that provide an infinite time guarantee of convergence [32–34]. Further references can be found in the reviews by Wakeham and Stateva [35] and by Segura et al. [36].

The use of guaranteed deterministic techniques comes at a computational cost, but they are particularly useful in difficult cases, or in cases where there are no external means of checking correctness, such as in parameter estimation [1]. In order to increase computational performance, a combination of local and global solvers is used to solve nonconvex subproblems in several guaranteed deterministic techniques, e.g., see [18,24,30]. The objective is to develop an algorithm for the solution of phase equilibrium, hereafter referred to as the PE algorithm, that guarantees convergence to the correct solution in finite time. The nonconvex subproblems are the tangent plane stability problem and the flash (or phase split) problem for a fixed number of phases. To guarantee that the correct solution of phase equilibrium has been found, it is necessary to use a deterministic global optimisation algorithm at least once during the PE algorithm, to solve the tangent plane stability test: if the proposed solution is found to be stable through this global test, the problem is solved and the PE algorithm can terminate. If it is found not to be stable, a flash problem must be solved for a fixed number of phases to generate a new solution, and a stability problem must eventually be solved to global optimality for a new potential phase configuration. The use of global optimisation for phase stability guarantees that when a final solution is reported by the PE algorithm, it is stable, i.e., the PE algorithm cannot converge to a wrong solution. This is not enough, however, to guarantee that the PE algorithm will find the stable solution in a finite time. For this, one must be able to guarantee that, for a given number of phases, the solution with the lowest Gibbs free energy is found. A local phase split algorithm is highly dependent on starting points and could converge repeatedly to a metastable solution, for example. In practice, this behaviour is often avoided by generating good initial points. Nevertheless, the only way to offer a theoretical guarantee of finite-time convergence is to ensure that global optimisation can be used to solve the flash problem; such an approach is implemented in GLOPEQ [24].

In the present work, we focus on the development of a guaranteed deterministic framework that can be applied to any equation of state (EOS), including those that are higher-than-cubic in volume such as the statistical associating fluid theory (SAFT) [37,38]. Higher-than-cubic EOSs are becoming increasingly popular due to their predictive capabilities for complex fluids, such as associating (i.e., hydrogen bonding) and polymer mixtures. When dealing with such approaches, which are typically formulated in the Helmholtz free energy $A(\underline{x}, V, T)$, where V is volume, the guaranteed solution of phase equilibrium is subject to additional difficulties. The Helmholtz free energy is the natural thermodynamic potential for developments within a statistical mechanical framework and has $\underline{x}$, V, T as natural variables, as opposed to $\underline{x}$, P, T for the Gibbs free energy. If the EOS is first-order in volume, then moving between the Helmholtz and Gibbs free energies is a trivial exercise. Unfortunately, this is only the case for the ideal gas EOS. For other EOSs, the evaluation of constant pressure properties requires a minimisation of the Gibbs free energy with respect to volume, with a constraint relating the volume to the pressure. This minimisation is often realised through the identification of all the volume roots of the EOS, and then the selection of the physically meaningful root (i.e., the most stable root, with the lowest Gibbs free energy). In the case of cubic equations of state, the volume roots of the EOS may be obtained analytically. For higher-than-cubic equations, calculations at a specified pressure and temperature are more time consuming, since the determination of $G(\underline{x}, P, T)$ at each point in composition requires the use of a nonlinear solver that can reliably identify the appropriate volume root for use in the calculation. In addition to increasing the cost of each Gibbs free energy evaluation, this inner minimisation can lead to complications when developing deterministic guaranteed approaches to fluid phase equilibrium. For instance, Xu et al. [30] have shown that the presence of an inner iteration can lead to large increases in the computational cost with a guaranteed deterministic algorithm. Though in the case of [30] the inner iteration is the system of equations arising from the association term of the SAFT approach [37,38], the solution of the pressure equation is also likely to lead to increases in computational cost: it is a low-dimensional but highly nonlinear problem. A promising avenue in this context is the formulation proposed by Nagarajan et al. [39,40], who developed a stability test and flash calculation method based on the Michelsen methodology, but using component molar densities as independent variables. This circumvents the need to solve for the volume roots of higher-than-cubic EOSs. It can also lead to enhanced robustness [19]. This formulation has been used successfully in an interval-based global optimisation algorithm to solve multi-component phase equilibria with a version of SAFT [30] and in a stochastic global optimisation algorithm [41].

Mitsos and Barton [27] have recently proposed an alternative approach to identifying a stable phase. They showed that the solutions of a dual formulation stemming from a single-phase Gibbs free energy minimisation problem, where mass balance constraints are imposed, are the stable equilibrium phases. This is an elegant new approach to the phase equilibrium problem, which requires no prior knowledge of the system being examined, neither in terms of the number of equilibrium phases present, nor in terms of the equilibrium phase compositions. At the solution of the dual problem, the composition of one of the stable equilibrium phases is obtained, as well as the equilibrium chemical potentials of all components. This information completely describes the common tangent plane connecting the equilibrium phases, and therefore may be used to find all other stable phases, which are in fact all the other (global) solutions of the dual problem. The dual approach has been applied to several case studies using the NRTL and UNIQUAC models and has been used in parameter estimation for a number of thermodynamic models [42,43]. Although the presence of a vapour phase is considered in [43], it is treated as ideal. In the solution algorithm proposed in [27] for the dual problem, one iterates between solving linear and nonconvex optimisation problems. The nonconvex problem has the same dimensionality as the tangent plane distance minimisation problem and a similar functional form. A feature of the dual approach is that it is not necessary to minimise the Gibbs free energy for different guesses of the number of phases. This approach has the potential to reduce the computational time required to solve the phase equilibrium problem provided that the number of iterations between the nonconvex and linear problems can be kept relatively low, and that, once a stable phase has been found, the remaining phases can be identified at low cost. This warrants further investigation and development for the case of general equations of state, particularly in the context of algorithms that identify all stable equilibrium phases.

In this paper, we develop a dual-based formulation of P, T phase equilibrium cast in the Helmholtz free energy and a guaranteed deterministic algorithm for its solution. The approach is general for any equation of state and any number of components. Instead of component molar densities [39], mole fractions and total molar

volume (or total molar density) are used as independent variables. The proposed algorithm is based on a combination of local and global solvers for the nonconvex subproblems, and guarantees that all stable phases can be found in finite time within a specified tolerance ϵ. It is particularly well-suited to higher-than-cubic equations of state formulated in the Helmholtz free energy, such as SAFT [37,38], because it does not require the explicit identification of volume roots in the calculation of the system properties at specified T and P. We focus on such EOSs in the application of the approach, and consider several challenging non-associating mixtures of two or three components as a means to demonstrate the basic ideas. The extension to associating systems is briefly mentioned in the conclusions.

In the next section, we introduce the concepts from thermodynamics and duality theory necessary to describe the approach, as well as the relevant notation. We review the framework of Mitsos and Barton [27], which is based on the dual of a Gibbs free energy minimisation problem. In Section 3, we reformulate the dual problem by expressing the Gibbs free energy in terms of the Helmholtz free energy, introducing the volume as an independent variable. The global solutions of this formulation are shown to be equivalent to those of [27], i.e., the global solutions characterise the stable phases present at equilibrium. In Section 4, we propose a deterministic algorithm for the guaranteed identification of all stable phases that makes minimal use of the more computationally expensive global optimisation solvers. In Section 5, we describe our prototype implementation and present computational results with two EOSs that are higher than cubic functions of volume: an AVDW (augmented van der Waals) and the SAFT-HS (statistical associating fluid theory for a hard sphere reference) EOS. We examine the phase behaviour of a number of binary and ternary systems, and show the effectiveness of the proposed approach in dealing with numerically challenging phase behaviour, such as that exhibited by highly asymmetric polymer–solvent systems. We use the examples to study the efficiency of the proposed algorithm, relative to an algorithm based solely on global optimisation for the nonconvex subproblems.

2. Background: phase stability and duality

We first review the underlying concepts necessary for the development of a formulation of the phase equilibrium problem in the composition-volume space.

2.1. Formulation of the phase equilibrium problem at constant temperature and pressure

This analysis is based on a system at constant temperature (T^0), pressure (P^0) and total mole numbers over all components ($\underline{n}^0$). Given these specifications, the most stable state of the system may be either one or multiple phases. The necessary and sufficient conditions for this most stable state are that it corresponds to the global minimum in the total Gibbs free energy function, G^T, over all phases, at the specified temperature (T^0) and pressure (P^0), subject to the conservation of mass. The total Gibbs free energy is defined as:

$$G^T(\underline{\mathbf{n}}, P^0, T^0) = \sum_{j=1}^{np}\sum_{i=1}^{nc} n_{i,j}\mu_{i,j}(\underline{n}_j, P^0, T^0), \tag{1}$$

where np is the number of phases present, nc is the number of components, $\underline{\mathbf{n}}$ is a matrix representing the number of moles of each component in each phase (i.e., $n_{i,j}$ is the number of moles of component i in phase j), $\underline{n}_j$ is the composition vector for phase j, and $\mu_{i,j}(\underline{n}_j, P^0, T^0)$ is the chemical potential of component i in phase j at the specified pressure and temperature (P^0, T^0) and composition of phase j. The mole numbers for each component must be such that,

$$\sum_{j=1}^{np} n_{i,j} = n_i^0, \quad i = 1, \ldots, nc. \tag{2}$$

The stable phase configuration may be found by global solution of the optimisation problem:

$$\begin{aligned} \min_{\underline{\mathbf{n}}, np} \quad & G^T(\underline{\mathbf{n}}, P^0, T^0) \\ \text{s.t.} \quad & \sum_{j=1}^{np} n_{i,j} - n_i^0 = 0, \quad i = 1, \ldots, nc. \end{aligned} \tag{3}$$

This optimisation problem is in a non-standard form in that the number of phases np, and hence the dimensionality of the matrix $\underline{\mathbf{n}}$, are unknown.

It is useful to define the intensive Gibbs free energy, $G(\underline{\hat{x}}_j, P, T)$, where $\underline{\hat{x}}_j$ denotes the vector of mole fractions in phase j:

$$G(\underline{\hat{x}}_j, P, T) = \sum_{i=1}^{nc} \hat{x}_{i,j}\mu_i(\underline{\hat{x}}_j, P, T). \tag{4}$$

Following Mitsos and Barton [27], we choose to work in mole fraction rather than mole number. It is also possible to develop the approach in the full space of nc components, by working with mole numbers. In the remainder of this article, we eliminate the mole fraction of component nc from vector $\underline{\hat{x}}_j$, by using the mass balance constraint in problem (3). We reformulate all functions in terms of the reduced variable vector $\underline{x}_j = (x_{j,1}, \ldots, x_{j,nc-1})^T$, so that Eq. (4) becomes

$$G(\underline{x}_j, P, T) = \left(\sum_{i=1}^{nc-1} x_{j,i}\mu_i(\underline{x}_j, P, T)\right) + \left(1 - \sum_{i=1}^{nc-1} x_{j,i}\right)\mu_{nc}(\underline{x}_j, P, T). \tag{5}$$

The intensive and total Gibbs free energies are related by

$$G^T(\underline{\mathbf{n}}, P^0, T^0) = \sum_{j=1}^{np} n_{Tj} G(\underline{x}_j, P^0, T^0), \tag{6}$$

where n_{Tj} is the number of moles in phase j.

The solution of the phase equilibrium problem (3) satisfies the necessary equilibrium conditions of equality of pressure and temperature over all phases, since the minimisation is carried out at constant T and P. The condition of equality of component chemical potentials over all phases is enforced as a result of the first-order optimality conditions. The Gibbs tangent plane criterion [44] states that the compositions corresponding to coexisting equilibrium phases (however many phases this may be) lie on a line that is tangent to the $G(\underline{x}, P^0, T^0)$ surface at each equilibrium phase composition. In addition, it states that the tangent plane running through the most stable equilibrium phase configuration (the global minimum in G^T) must remain below the $G(\underline{x}, P^0, T^0)$ surface throughout the whole composition space. Thus, this plane is a supporting hyperplane of $G(\underline{x}, P^0, T^0)$ in the composition space and it is tangent to $G(\underline{x}, P^0, T^0)$ at the compositions of all of the stable phases. The gradient of the tangent plane to the $G(\underline{x}, P^0, T^0)$ surface for a phase j, at composition $\underline{x}_j$, yields the vector of component chemical potentials in that phase [45]:

$$\begin{aligned} &\mu_{i,j}(\underline{x}_j, P^0, T^0) - \mu_{nc,j}(\underline{x}_j, P^0, T^0) \\ &= \left(\frac{\partial G(\underline{x}_j, P^0, T^0)}{\partial x_{i,j}}\right)_{x_{k,j;k=1,\ldots,nc-1,k\neq i}, P, T}, \quad i = 1, \ldots, nc-1;\ j = 1, \ldots, np. \end{aligned} \tag{7}$$

Since all stable phases lie on this common tangent, there must be equality of chemical potential between phases. When np is

not known a priori, phase equilibrium (problem (3) or an equivalent formulation) is usually solved iteratively following the general scheme of Michelsen [6,7], by alternating between a stability test and the solution of phase equilibrium for a fixed number of phases. This results in a series of optimisations in $nc-1$ (or nc) variables for phase stability and $np \times nc$ variables for phase equilibrium (where np varies from iteration to iteration). The dimensionality of the latter problem can be reduced by eliminating one phase or one component from the formulation using the material balance constraint. Clearly, the computational effort required to solve the phase equilibrium problem for a fixed number of phases increases with the number of phases and components. This has an impact on computational performance especially for guaranteed deterministic algorithms. In this case, the nonconvex phase stability problem must be solved to global optimality at least once to prove the stable phases have been found. In addition, the phase equilibrium may need to be solved to global optimality to offer a guarantee of convergence to the global solution: for a given number of phases, it may not be possible with a local solver to identify a phase split with a lower Gibbs free energy than the current (unstable) minimum. In this case, it is necessary to use a global solver to determine whether (i) a better solution exists, or (ii) the specified number of phases is not stable.

2.2. Basic concepts of duality theory

The main concepts of duality theory needed for the development of the problem formulation are explained in this section. An excellent introduction to duality theory is given in [46]. We consider a minimisation problem with a nonlinear objective function and linear equality constraints, as the phase equilibrium problem fits within this class:

$$\begin{aligned} \min_{\underline{x}\in X} \quad & f(\underline{x}) \\ \text{s.t.} \quad & h_i(\underline{x}) = 0, \quad i = 1,\ldots,m \\ & \underline{x} \in X \in \mathbb{R}^n \end{aligned} \tag{8}$$

where $f(\underline{x})$ is the objective function to be minimised, $\underline{x}$ is the n-dimensional vector of optimisation variables, $h_i(\underline{x})$ is the ith equality constraint, m is the number of equality constraints ($n \geq m$), and X is a closed set. We assume that the set $\mathcal{H} = \{\underline{x} : \underline{h}(\underline{x}) = \underline{0}, \underline{x} \in X\}$ is non-empty, i.e., that there exists a feasible solution to problem (8). In the context of duality theory, this problem is the *primal problem* and its *Lagrangian dual problem* can be expressed as[1] [46]:

$$\sup_{\underline{\lambda}} \theta(\underline{\lambda}) \tag{9}$$

where:

$$\theta(\underline{\lambda}) = \inf_{\underline{x}\in X} L(\underline{\lambda}, \underline{x}) \tag{10}$$

$$= \inf_{\underline{x}\in X} [f(\underline{x}) + \underline{\lambda}^T \underline{h}(\underline{x})], \tag{11}$$

where $\underline{\lambda}$ is the vector of Lagrange multipliers associated with the constraint vector $\underline{h}(\underline{x}) = \underline{0}$ and $L(\underline{x}, \underline{\lambda})$ is the Lagrangian dual function. The dual formulation consists of an inner minimisation with respect to $\underline{x}$ and an outer maximisation with respect to $\underline{\lambda}$.

The dual problem may be interpreted geometrically by considering the Lagrangian function for a problem with only one constraint, $h(\underline{x}) = 0$, and hence a single multiplier λ:

$$L(\underline{x}, \lambda) = f(\underline{x}) + \lambda h(\underline{x}). \tag{12}$$

[1] The supremum of a set S (sup (S)) is defined as its least upper bound and the infimum (inf (S)) as its greatest lower bound; see for example, [47].

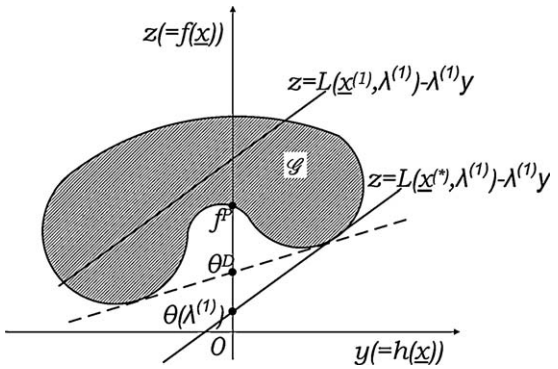

Fig. 1. The geometrical interpretation of a Lagrangian dual problem for a one-dimensional problem with one linear constraint (adapted from [46]).

Let us define a plane y–z in which $h(\underline{x})$ is plotted on the y-axis and $f(\underline{x})$ on the z-axis, as shown in Fig. 1, where the set $\mathcal{G}$ represents all combinations of values of the objective function and the constraint $(h(\underline{x}), f(\underline{x}))$ for $\underline{x} \in X$. Thus, $\mathcal{G}$ is the image of X under the (h, f) map and is given by $\mathcal{G} = \left\{(y, z) : y = h(\underline{x}), z = f(\underline{x}), \underline{x} \in X\right\}$.

The intersection of the z-axis with $\mathcal{G}$ gives the set of values of $f(\underline{x})$ for all *feasible* values of $\underline{x}$, i.e., for all $\underline{x} \in X$ such that $y = h(\underline{x}) = 0$. At the solution of the primal problem, the equality constraint must be satisfied, which implies the solution lies on the z-axis. Since $f(\underline{x})$ must reach its minimum value at the solution of the primal problem, the solution must also lie on the lower boundary of set $\mathcal{G}$. Thus, the solution of the primal problem is the point at which the lower boundary of $\mathcal{G}$ intersects the z-axis. This point is labelled f^P in Fig. 1.

To interpret the dual formulation and its link to the primal problem, we first consider given values of $\underline{x}^{(1)} \in X$ and $\lambda^{(1)}$ and the line defined by:

$$z = L(\underline{x}^{(1)}, \lambda^{(1)}) - \lambda^{(1)} y, \tag{13}$$

which has slope $-\lambda^{(1)}$ and intersects the z-axis at $L(\underline{x}^{(1)}, \lambda^{(1)})$. Since $\underline{x}^{(1)}$ has been chosen within the set X, it can be seen from Eqs. (12) and (13) that line (13) and the set $\mathcal{G}$ share at least one point, $(y, z) = (h(\underline{x}^{(1)}), f(\underline{x}^{(1)}))$. By changing the value of $\underline{x}$ while keeping $\lambda^{(1)}$ constant, line (13) may be moved in the y–z plane to change its intercept while maintaining a constant slope, as shown in Fig. 1. Based on Eq. (10), to evaluate $\theta(\lambda^{(1)})$, $L(\underline{x}, \lambda^{(1)})$ must be minimised with respect to $\underline{x}$ over X. This is equivalent to finding a value of x, x^*, that gives the minimum intercept of line (13) with the z-axis, $\theta(\lambda^{(1)}) = L(\underline{x}^*, \lambda^{(1)})$. By definition, this line must maintain contact with the set $\mathcal{G}$, and therefore must be a supporting tangent to $\mathcal{G}$. Solving the dual problem (9) is then equivalent to finding the value of λ such that the intercept $\theta(\lambda)$ of the supporting tangent with the z-axis is maximal. This tangent is shown as a dashed line in Fig. 1 and the solution of the dual problem is denoted by θ^D. In cases where the set $\mathcal{G}$ is convex, the solution of the dual problem, θ^D, is equal to that of the primal problem, f^P. When $\mathcal{G}$ is nonconvex, however, there may be a difference between the two values, as shown in Fig. 1. This is referred to as the duality gap. By construction, the solutions of the primal and dual problems are always such that $f^P \geq \theta^D$. In a multidimensional problem, the solution of the dual problem is a supporting hyperplane of the set $\mathcal{G}$ over X [46].

An important property of the dual function in (9) is that it is concave in $\underline{\lambda}$, so that the local maximisation of $\theta(\underline{\lambda})$ yields the global optimum solution. The practical solution of the dual formulation is however complicated by the need to perform an inner minimisation with respect to $\underline{x}$ for each evaluation of $\theta(\underline{\lambda})$. If the objective function $f(\underline{x})$ is nonconvex and/or the equality constraints $\underline{h}(\underline{x})$ are nonlinear, then the inner minimisation may have local as well as global solutions.

2.3. Phase stability as a dual problem

Phase stability may be posed as a constrained optimisation problem and the resulting link between phase stability and Lagrange multipliers, in various thermodynamic spaces, is well-recognised [48]. In this context, it is interesting to note that Mcdonald and Floudas [21,22,49] use relaxed Lagrangian dual problems to determine phase stability in a guaranteed manner for the NRTL and UNIQUAC models. Mitsos and Barton [27] have shown that one of the stable phases of a mixture at given total composition, temperature and pressure can be determined by solving a Lagrangian dual optimisation problem to global optimality. This is closely related to the minimisation of the tangent plane distance. Furthermore, they have shown that the solution of the dual problem in fact characterises all the stable phases at the given conditions. This dual formulation is described here.

2.3.1. Formulation of the dual problem

The derivation of the dual formulation starts by defining an optimisation problem, or primal problem, that is related to the phase equilibrium problem:

$$\begin{aligned} \min_{\underline{x}} \quad & G(\underline{x}, P^0, T^0) \\ \text{s.t.} \quad & x_i^0 - x_i = 0, \quad i = 1, \ldots, nc-1 \\ & \underline{x} \in X \subset \mathbb{R}^{nc-1} \end{aligned} \tag{P_x}$$

The set X is given by $\{\underline{x} : \underline{x} \in [0,1]^{nc-1}\}$. It is assumed that G is a continuous, but not necessarily differentiable, function of $\underline{x}$, that more than one component are present ($nc > 1$), and that the overall composition is such that $x_i^0 > 0$ for all $i = 1, \ldots, nc-1$.

The solution of the primal problem (P_x) is much simpler than that of the phase equilibrium problem (3). In problem (3), the Gibbs free energy is calculated over all (i.e., potentially multiple) phases. By contrast, the primal objective function here is the Gibbs free energy of the system in a single-phase state and, given the mass balance constraint, the solution of the primal is trivially equal to the total composition. The optimal objective function value is $G^P = G(\underline{x}^0, P^0, T^0)$. The solution of the primal problem corresponds simply to an evaluation of the $G(\underline{x}, P^0, T^0)$ function at the overall composition $\underline{x}^0$.

A dual problem (D_x) corresponding to this primal problem is given by[2]:

$$\begin{aligned} G^D = \max_{\underline{\lambda} \in \mathbb{R}^{nc-1}} \quad & \theta(\underline{\lambda}) \\ \text{s.t.} \quad & \theta(\underline{\lambda}) = \min_{\underline{x} \in X} L(\underline{x}, \underline{\lambda}), \end{aligned} \tag{D_x}$$

where $L(\underline{x}, \underline{\lambda})$ is the Lagrangian of (P_x),

$$L(\underline{x}, \underline{\lambda}) = G(\underline{x}, P^0, T^0) + \sum_{i=1}^{nc-1} \lambda_i (x_i^0 - x_i), \tag{14}$$

λ_i is the Lagrange multiplier for the equality constraint on the mole fraction of component i in problem (P_x), and $\theta(\underline{\lambda})$ is the dual function.

2.3.2. Equivalence between the dual problem and phase stability

In this section, some of the key ideas behind the dual problem formulation are discussed; the reader is referred to [27] for a more detailed treatment. In particular, an exhaustive proof that the global solutions of problem (D_x) correspond to stable equilibrium phases is given in [27].

Firstly, we should recall the meaning of 'phase stability' in the (N, P, T) ensemble. A phase (or a configuration of multiple phases, e.g., two liquid phases and one vapour phase, in equilibrium) is stable if and only if the system is in a configuration that minimises its total Gibbs free energy, as given by Eq. (6). The exact nature of the most stable configuration of a system depends on the convexity of the $G(\underline{x}, P^0, T^0)$ surface. The convex hull (or convex envelope) of a function $f(x)$ may be defined as the function that is the tightest convex underestimator of $f(x)$ (e.g. [46,50]). The most stable phase configuration of a system lies on the convex hull of the $G(\underline{x}, P^0, T^0)$ surface. The convex hull of $G(\underline{x}, P^0, T^0)$ is a combination of the function itself and supporting hyperplane(s), tangential to $G(\underline{x}, P^0, T^0)$ at the compositions of the stable phases. Thus, if the total (or feed) composition $\underline{x}^0$ of the mixture lies in a region where $G(\underline{x}, P^0, T^0)$ and its convex hull are equal, the phase with composition $\underline{x}^0$ is stable. If $\underline{x}^0$ lies in a region where the convex hull strictly underestimates the $G(\underline{x}, P^0, T^0)$ function, the phase with composition $\underline{x}^0$ is unstable or metastable and there is a phase split. When the $G(\underline{x}, P^0, T^0)$ surface is convex over the whole composition range, the system remains in a single phase, whatever its composition. A graphical representation of $G(\underline{x}, P^0, T^0)$ and its convex hull is presented in Fig. 2. Solving the phase equilibrium problem involves identifying the convex hull of the $G(\underline{x}, P^0, T^0)$ function at $\underline{x}^0$.

Comparing the convex hull of the $G(\underline{x}, P^0, T^0)$ surface and the surface itself is another way of stating the tangent plane criterion [44], which can be used to determine whether, at constant temperature T^0 and pressure P^0 a phase at a given composition $\underline{x}^0$ is stable. The criterion requires that if the tangent to the $G(\underline{x}, P^0, T^0)$ surface, taken at $\underline{x}^0$ lies below the $G(\underline{x}, P^0, T^0)$ surface at all compositions, then the state with composition $\underline{x}^0$ is a stable phase. This is equivalent to determining whether $G(\underline{x}^0, P^0, T^0)$ lies on the convex hull of $G(\underline{x}, P^0, T^0)$. Furthermore, at a multiphase stable equilibrium

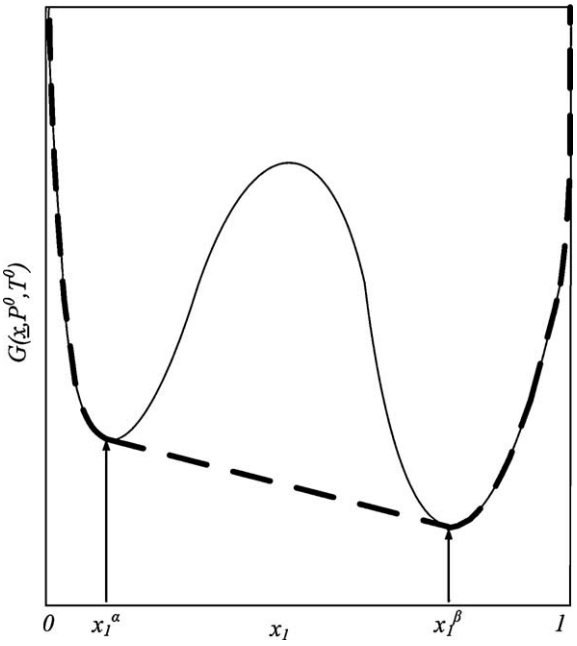

Fig. 2. A sketch of $G(\underline{x}, P^0, T^0)$ and its convex hull as a function of x_1 for a binary system that exhibits liquid–liquid separation. $G(\underline{x}, P^0, T^0)$ is shown as a thin continuous curve, and the convex hull as a thick dashed curve. If $x_1^0 < x_1^\alpha$ or $x_1^0 > x_1^\beta$, $G(\underline{x}, P^0, T^0)$ is equal to its convex hull, therefore the stable configuration is a single phase of composition $\underline{x}^0$. A system with a total composition $x_1^0 \in [x_1^\alpha, x_1^\beta]$ is unstable or metastable, as $G(\underline{x}, P^0, T^0)$ is strictly underestimated by its convex hull. It therefore separates into two phases of compositions $\underline{x}^\alpha$ and $\underline{x}^\beta$.

[2] max and min, rather than sup and inf are used in this definition of the dual problem. The reader is referred to propositions 13 and 16 of [27] for proofs that a maximum of D_x and a minimum of the inner problem are attained, when subject to suitable assumptions.

state, the chemical potential of each component must be the same in all phases, so that the derivatives of the $G(\underline{x}, P^0, T^0)$ surface must be identical at all of the stable phase compositions. Therefore, the tangent to the $G(\underline{x}, P^0, T^0)$ surface, taken at one of the stable phase compositions, is tangential to the $G(\underline{x}, P^0, T^0)$ surface at the compositions of all the other phases in this multiphase configuration.

To link the tangent plane criterion to the dual problem, we denote the partial derivative of $G(\underline{x}, P^0, T^0)$ with respect to some mole fraction x_i at some composition $\underline{x}^S$ by

$$g_i^S = \left(\frac{\partial G(\underline{x}^S, P^0, T^0)}{\partial x_i} \right)_{x_{j\neq i, j=1,\ldots,nc-1}, P, T}, \quad \text{for } i = 1, \ldots, nc-1. \tag{15}$$

Let us consider that the phase composition $\underline{x}^S$ is stable and write the equation of the tangent plane, $G_T(\underline{x}, P^0, T^0; \underline{x}^S)$, to the $G(\underline{x}, P^0, T^0)$ surface at $\underline{x}^S$:

$$G_T(\underline{x}, P^0, T^0; \underline{x}^S) = G(\underline{x}^S, P^0, T^0) + \sum_{i=1}^{nc-1} g_i^S (x_i - x_i^S). \tag{16}$$

Since $\underline{x}^S$ is stable, then the following must hold:

$$G_T(\underline{x}, P^0, T^0; \underline{x}^S) \leq G(\underline{x}, P^0, T^0), \quad \forall x \in X, \tag{17}$$

i.e., $G_T(\underline{x}, P^0, T^0; \underline{x}^S)$ is a supporting hyperplane of $G(\underline{x}, P^0, T^0)$ over X.

By generalising the geometric discussion of duality in Section 2.2, it can be seen that the supporting hyperplane at the solution $(\underline{x}^*, \underline{\lambda}^*)$ of the dual problem (D_x) is given by

$$z = L(\underline{x}^*, \lambda^*) - \sum_{i=1}^{nc-1} \lambda_i^* (x_i^0 - x_i). \tag{18}$$

Introducing the definition of L, this can be rewritten as

$$z = G(\underline{x}^*, P^0, T^0) + \sum_{i=1}^{nc-1} \lambda_i^* (x_i - x_i^*). \tag{19}$$

By comparing Eqs. (16) and (19), it can be seen that the supporting hyperplanes arising from the tangent plane criterion and from the solution of the dual problem are identical provided that $\underline{x}^*$ is the composition of the one of the stable phases and that $\lambda_i^* = g_i$, $i = 1, \ldots, nc-1$. Mitsos and Barton [27] have proved this equivalence. In particular, they have shown that

1. Any global solution $(\underline{x}^*, \underline{\lambda}^*)$ of the dual problem describes a supporting hyperplane of the $G(\underline{x}, P^0, T^0)$ surface over X. This hyperplane has a gradient of $\underline{\lambda}^*$ and passes through the point $\underline{x}^*, G(\underline{x}^*, P^0, T^0)$.
2. The total composition of the mixture $\underline{x}^0$ lies in the convex hull of the set X^* of composition vectors at the global solutions, so that there exists a combination of the composition vectors in X^* that satisfies the mass balance constraint in problem (3).
3. $(\underline{x}^*, \underline{\lambda}^*)$ is a solution of the dual problem if and only if it characterises one of the stable equilibrium phases.

Indeed, the inner problem can be linked to the phase stability problem at the overall composition by choosing $\lambda_i^0 \equiv (\partial G(\underline{x}^0, P^0, T^0)/\partial x_i)_{T,P,x_{k\neq i}}$. In this case, the objective function is the tangent plane distance, offset by a constant $\lambda_i^0 x_i^0$. Under these conditions, the solution of the inner problem is equivalent to the minimisation of the tangent plane distance, as carried out by, for example, Michelsen [6], McDonald and Floudas [21–23,49], Harding and Floudas [25] and Hua et al. [18,28]. In the context of the dual optimisation approach discussed here, if the global solution of the inner problem is G^P for this choice of λ_i value, then $\underline{x}^0$ is stable, regardless of whether $\underline{x}^0$ is reported as the only global solution of the problem.

3. The phase equilibrium problem as a dual problem in volume and composition

3.1. The Gibbs free energy as a function of volume

As mentioned in the introduction, the natural variables of the Gibbs free energy function are $(\underline{x}, P, T)$, but equations of state are almost invariably explicit functions of volume rather than pressure. There are some advantages in working with the Helmholtz free energy, as highlighted in [19,30,39,41]. In the context of constant pressure phase equilibrium calculations using higher-than-cubic equations of state, robustness and speed improvements may be achieved by removing the need to solve the pressure constraint $P(\underline{x}, V, T) = P^0$ at each step in the calculation. For non-guaranteed solution methods, the use of a nonlinear solver at each evaluation of the Gibbs free energy can be expected to consume a significant proportion of the solution time. For a guaranteed method, the presence of an inner iteration makes it difficult to deploy deterministic branch-and-bound methods such as BARON [51,52] or αBB [53,54].

The alternative formulation proposed by Nagarajan et al. [39,40] overcomes these issues by recasting the Gibbs free energy minimisation and the tangent plane criterion in terms of component molar densities so that the pressure constraint is satisfied at the solution of the problem without being solved explicitly. In this section, we show how a formulation in the volume-composition space can be deployed within the dual framework of [27]. This provides the theoretical basis for a practical implementation of this framework for general equations of state.

Firstly, we recall a thermodynamic expression that will be central to this discussion, the relationship between the Gibbs and the Helmholtz free energies:

$$G(\underline{x}, P(\underline{x}, V, T^0), T^0) = A(\underline{x}, V, T^0) + P(\underline{x}, V, T^0)V, \tag{20}$$

where P is pressure, V is molar volume and $A(\underline{x}, V, T^0)$ is the Helmholtz free energy at a fixed temperature T^0. The standard thermodynamic relation between molar volume and pressure is

$$P(\underline{x}, V, T) = -\left(\frac{\partial A}{\partial V} \right)_{\underline{x}, T}. \tag{21}$$

It may be observed from Eqs. (20) and (21) that the value of G at a given composition, pressure and temperature may not be unique if the EOS has more than one volume root, i.e., there may be more than one value of V that satisfies Eq. (21). When multiple volume roots exist, we must select that which yields the lowest value of G as the physically meaningful value of V. This implies that $G(\underline{x}, P^0, T^0)$ must in fact be minimised with respect to the implicit variable volume, i.e.,

$$\begin{aligned} G(\underline{x}, P^0, T^0) = \min_{V>0} \quad & [A(\underline{x}, V, T^0) + P^0 V] \\ \text{s.t.} \quad & P^0 = -\left(\frac{\partial A}{\partial V} \right)_{\underline{x}, T}. \end{aligned} \tag{22}$$

As noted by Nagarajan et al. [39,40] (in the space of mole numbers), a stationary point of the unconstrained problem

$$\min_{V>0} [A(\underline{x}, V, T^0) + P^0 V] \tag{23}$$

satisfies the optimality conditions for the constrained problem (22). Indeed, the first-order optimality condition of problem (23), that the first derivative of the objective function with respect to V must be equal to zero, means that at the solution, the pressure is equal

to P^0:

$$\left.\frac{\partial(A(\underline{x},V,T^0)+P^0V)}{\partial V}\right|_{\underline{x},T} = \left.\frac{\partial A(\underline{x},V,T^0)}{\partial V}\right|_{\underline{x},T} + P^0 = 0. \quad (24)$$

Using Eq. (21), this is equivalent to

$$P(\underline{x}^*,V^*,T^0) = P^0, \quad (25)$$

where $(\underline{x}^*, V^*)$ denotes the solution of problem (23). Since the objective functions for problems (22) and (23) are identical, the solution of problem (23) is also a solution of problem (22).

Returning now to the formulation of phase equilibrium as a dual problem, we present our main result, namely how this framework can be used to tackle the P, T phase equilibrium problem when using complex EOSs. By working with the Helmoltz free energy in the space of its natural variables and exploiting the properties of branch-and-bound algorithms, we develop in Section 4 a solution algorithm that is guaranteed to find all stable phases.

3.2. Incorporating volume into the dual formulation

The result described by Eq. (25) may be employed to reformulate the dual problem (D_x) to avoid solving explicitly for the volume roots of the EOS when evaluating the Lagrangian function. We consider the following primal problem:

$$\begin{aligned} \min_{\underline{x},V}\ & A(\underline{x},V,T^0)+P^0V \\ \text{s.t.}\ & x_i^0 - x_i = 0 \quad i=1,\ldots,nc-1 \\ & \underline{x}\in X\subset\mathbb{R}^{nc-1} \\ & V\in[\underline{V},\overline{V}], \end{aligned} \quad (P_{x,V})$$

where we assume, without loss of generality that physical bounds for the volume V are set so that $V\in[\underline{V},\overline{V}]$. In the examples we present, we work in packing fraction rather than volume: these two spaces are mathematically equivalent (see Appendix A), and an upper bound for the packing fraction is provided by the close-packing limit of hard spheres.

In developing a formulation of the phase equilibrium problem in the space of component molar densities, Nagarajan et al. [39,40] note that the linear mass balance constraints become bilinear. In problem ($P_{x,V}$), because a single phase is considered, the mass balance constraint remains linear. This is a useful feature in the context of guaranteed deterministic methods, as it removes one source of nonconvexity in the formulation. From problem ($P_{x,V}$), we can formulate a dual problem as

$$\begin{aligned} \max_{\underline{\lambda}\in\mathbb{R}^{nc-1}}\ & \theta^V(\underline{\lambda}) \\ \text{s.t.}\ & \theta^V(\underline{\lambda}) = \min_{\underline{x}\in X,V\in[\underline{V},\overline{V}]} L^V(\underline{x},V,\underline{\lambda}) \\ & \qquad \text{where}\quad L^V(\underline{x},V,\underline{\lambda}) = A(\underline{x},V,T^0)+P^0V \\ & \qquad\quad + \sum_{i=1}^{nc-1}\lambda_i(x_i^0-x_i). \end{aligned} \quad (D_{x,V})$$

We show that the inner problem of the dual in the x space for a given $\underline{\lambda}^k$,

$$\min_{\underline{x}\in X} L(\underline{x},\underline{\lambda}^k) = \min_{\underline{x}\in X}\left(G(\underline{x},P^0,T^0)+\sum_{i=1}^{nc-1}\lambda_i^k(x_i^0-x_i)\right), \quad (IP_x)$$

and the inner problem of the dual in the x–V space for the same $\underline{\lambda}^k$,

$$\begin{aligned} &\min_{\underline{x}\in X,V\in[\underline{V},\overline{V}]} L^V(\underline{x},V,\underline{\lambda}^k) \\ &= \min_{\underline{x}\in X,V\in[\underline{V},\overline{V}]}\left(A(\underline{x},V,T^0)+P^0V+\sum_{i=1}^{nc-1}\lambda_i^k(x_i^0-x_i)\right), \end{aligned} \quad (IP_{x,V})$$

have the same solution.

Firstly, the first-order optimality conditions for the unconstrained optimisation problem of (IP_x) are examined. They dictate that at the solution $\tilde{\underline{x}}$, the partial derivative of L with respect to each component of $\underline{x}$ must be zero:

$$\left(\frac{\partial L(\tilde{\underline{x}},\underline{\lambda})}{\partial x_i}\right)_{P,T,\underline{\lambda},x_{k\neq i,k=1,\ldots,nc-1}} = 0, \quad i=1,\ldots,nc-1, \quad (26)$$

so that,

$$\left(\frac{\partial G(\tilde{\underline{x}},P^0,T^0)}{\partial x_i}\right)_{P,T,\underline{\lambda},x_{k\neq i,k=1,\ldots,nc-1}} = \lambda_i, \quad i=1,\ldots,nc-1. \quad (27)$$

Thus, by combining Eqs. (7) and (27), it can be seen that, at the solution to the minimisation problem, the undetermined multiplier λ_i is related to the chemical potential of component i by

$$\lambda_i = \mu_i(\tilde{\underline{x}},P^0,T^0) - \mu_{nc}(\tilde{\underline{x}},P^0,T^0), \quad i=1,\ldots,nc-1. \quad (28)$$

Next, we conduct the same analysis on the first-order optimality conditions for the proposed formulation in volume, problem ($IP_{x,V}$). The first-order derivatives of L^V with respect to both $\underline{x}$ and the additional variable V must be equal to 0 at the solution $(\underline{x}^*, V^*)$:

$$\begin{aligned} \left(\frac{\partial L^V(\underline{x}^*,V^*,\underline{\lambda})}{\partial V}\right)_{\underline{x},T} &= \left(\frac{\partial A(\underline{x}^*,V^*,T^0)}{\partial V}\right)_{\underline{x},T} + P^0 \\ &= -P(\underline{x}^*,V^*,T^0)+P^0 = 0, \end{aligned} \quad (29)$$

and

$$\left(\frac{\partial L^V(\underline{x}^*,V^*,\underline{\lambda})}{\partial x_i}\right)_{x_{k\neq i},V,T,\underline{\lambda}} = \left(\frac{\partial A(\underline{x}^*,V^*,T^0)}{\partial x_i}\right)_{x_{k\neq i},V,T} - \lambda_i = 0, \quad i=1,\ldots,nc-1. \quad (30)$$

The first relation, Eq. (29), ensures that the pressure is equal to the specified P^0 at the solution of the inner problem in the x–V space. This requirement is trivially met at the solution of the inner problem in the x space, since G is calculated at P^0. The second equation, Eq. (30), relates the Lagrange multiplier λ_i to the chemical potential of component i. This relation is now expressed in terms of the Helmholtz free energy at constant volume, rather than the Gibbs free energy at constant pressure. Next, we show that the two conditions are in fact equivalent at the solution of the inner problem in the x–V space.

We begin by defining a function of volume and composition at constant temperature $\bar{G}(\underline{x},V,T^0)$ where,

$$\bar{G}(\underline{x},V,T^0) = A(\underline{x},V,T^0)+P^0V. \quad (31)$$

Then,

$$d\bar{G}(\underline{x},V,T^0) = \sum_{i=1}^{nc-1}\left(\frac{\partial\bar{G}}{\partial x_j}\right)_{x_{k\neq i},V,T} dx_i + \left(\frac{\partial\bar{G}}{\partial V}\right)_{\underline{x},T} dV. \quad (32)$$

Given the relation $P=P(\underline{x},V,T)$, the partial derivative of $\bar{G}$ with respect to x_i, at constant $x_{k\neq i}$, P, T, is given by

$$\left(\frac{\partial\bar{G}}{\partial x_i}\right)_{x_{k\neq i},P,T} = \left(\frac{\partial\bar{G}}{\partial x_i}\right)_{x_{k\neq i},V,T} + \left(\frac{\partial\bar{G}}{\partial V}\right)_{\underline{x},T}\left(\frac{\partial V}{\partial x_i}\right)_{x_{k\neq i},P,T}. \quad (33)$$

The left-hand side of Eq. (33) is equal to the partial derivative of $G(\underline{x},P,T)$ with respect to x_i. Using this and the definition of $\bar{G}$ in Eq. (31),

$$\left(\frac{\partial G(\underline{x},P,T)}{\partial x_i}\right)_{x_{k\neq i},P,T}=\left(\frac{\partial A(\underline{x},V,T^0)}{\partial x_i}\right)_{x_{k\neq i},V,T}+\left[\left(\frac{\partial A(\underline{x},V,T^0)}{\partial V}\right)_{\underline{x},T}+P^0\right]\left(\frac{\partial V}{\partial x_i}\right)_{x_{k\neq i},P,T}. \quad (34)$$

But from Eq. (29), at the solution $(\underline{x}^*, V^*)$ of the inner problem in the x–V space,

$$\left(\frac{\partial A(\underline{x}^*,V^*,T^0)}{\partial V}\right)_{\underline{x},T}=-P(\underline{x}^*,V^*,T^0)=-P^0, \quad (35)$$

so that, at the solution, Eq. (34) becomes

$$\left(\frac{\partial G(\underline{x}^*,P^0,T^0)}{\partial x_i}\right)_{x_{k\neq i},P,T}=\left(\frac{\partial A(\underline{x}^*,V^*,T^0)}{\partial x_i}\right)_{x_{k\neq i},V,T}. \quad (36)$$

This implies that

$$\left(\frac{\partial L^V(\underline{x}^*,V^*,\underline{\lambda})}{\partial x_i}\right)_{x_{k\neq i},V,T,\underline{\lambda}}=\left(\frac{\partial L(\underline{x}^*,\underline{\lambda})}{\partial x_i}\right)_{x_{k\neq i},P,T,\underline{\lambda}}=0,\quad i=1,\ldots,nc-1. \quad (37)$$

Since $(\underline{x}^*, V^*)$ satisfies $P(\underline{x}^*, V^*, T^0) = P^0$, Eq. (37) leads us to conclude that $(\underline{x}^*, V^*)$ is a stationary point of $(IP_{x,V})$, the inner problem in the x–V (Helmholtz) space, for a given $\underline{\lambda}$ if and only if $\underline{x}^*$ is a stationary point of (IP_x), the inner problem in the x (Gibbs) space for this $\underline{\lambda}$. V^* is the physical volume root corresponding to $\min_{V\in[\underline{V},\overline{V}]} G(\underline{x}^*, P^0(\underline{x}^*, V, T^0), T^0)$. The fact that the objective functions of problems (IP_x) and $(IP_{x,V})$ are equal whenever the physical volume root is used ensures that a stationary point of (IP_x) is a minimum if and only if the corresponding stationary point of $(IP_{x,V})$ is also a minimum.

Since the inner problems in the x and x–V spaces are equivalent, so are the dual problems (D_x) and $(D_{x,V})$ in the x and x–V spaces. Consequently, the proof in [27] that the global solution of problem (D_x) is a stable equilibrium phase may equally be applied to problem $(D_{x,V})$.

3.3. The solution of the dual is a supporting hyperplane of the Helmholtz free energy

The solution of dual $(D_{x,V})$ defines a supporting hyperplane of $G(\underline{x}, P^0, T^0)$ over X, as does the solution of dual (D_x). Interestingly, it may also be shown that the solution of the dual in the composition and volume space $(D_{x,V})$, and therefore the solution of the P, T phase equilibrium problem, also defines a supporting hyperplane of $A(\underline{x}, V, T^0)$ over $X\times[\underline{V},\overline{V}]$. This is achieved by following the proof of [27] that the solution of the dual (D_x) defines a supporting hyperplane of $G(\underline{x}, P^0, T^0)$ over X.

Consider a solution $(\underline{x}^*, V^*)$ of $(IP_{x,V})$ for some $\underline{\lambda}=\underline{\lambda}^*$. The Lagrangian L^V evaluated at this solution is as follows:

$$L^V(\underline{x}^*,V^*,\underline{\lambda}^*)=A(\underline{x}^*,V^*,T^0)+P^0V^*+\sum_{i=1}^{nc-1}\lambda_i^*(x_i^0-x_i^*). \quad (38)$$

Since $(\underline{x}^*, V^*)$ minimises $L(\underline{x}, V, \underline{\lambda}^*)$ over all $\underline{x}\in X$ and $V>0$, we can say that

$$L^V(\underline{x}^*,V^*,\underline{\lambda}^*)\le L(\underline{x},V,\underline{\lambda}^*),\quad \forall\underline{x}\in X, V\in[\underline{V},\overline{V}], \quad (39)$$

and therefore that

$$A(\underline{x}^*,V^*,T^0)+P^0V^*+\sum_{i=1}^{nc-1}\lambda_i^*(x_i^0-x_i^*)\le A(\underline{x},V,T^0)+P^0V+\sum_{i=1}^{nc-1}\lambda_i^*(x_i^0-x_i),\quad \forall\underline{x}\in X, V\in[\underline{V},\overline{V}]. \quad (40)$$

Rearrangement of Eq. (40) yields:

$$A(\underline{x}^*,V^*,T^0)+P^0(V^*-V)+\sum_{i=1}^{nc-1}\lambda_i^*(x_i-x_i^*)\le A(\underline{x},V,T^0),\quad \forall\underline{x}\in X, V\in[\underline{V},\overline{V}], \quad (41)$$

or equivalently, by making use of the first-order optimality conditions (29) and (30),

$$A(\underline{x}^*,V^*,T^0)+\left(\frac{\partial A}{\partial V}\right)_{\underline{x},T}(V-V^*)+\sum_{i=1}^{nc-1}\left(\frac{\partial A}{\partial x_i}\right)_{x_{k\neq i},V,T}(x_i-x_i^*)\le A(\underline{x},V,T^0),\quad \forall\underline{x}\in X, V\in[\underline{V},\overline{V}], \quad (42)$$

where the derivatives are evaluated at $(\underline{x}^*, V^*, T^0)$. This proves that the solution $(\underline{x}^*, V^*)$ defines a hyperplane that supports $A(\underline{x}, V, T^0)$ over $X\times[\underline{V},\overline{V}]$ and that is tangent to $A(\underline{x}, V, T^0)$ at $(\underline{x}^*, V^*)$, the composition and volume of a stable phase.

3.4. From phase stability to stable phase equilibrium

Once a global solution of the dual problem $(D_{x,V})$ has been found, the optimal Lagrange multiplier vector $\underline{\lambda}^*$ is known, as are the chemical potentials of all the components μ_i^*, the composition and volume of one stable phase $\underline{x}^*$, V^*, and the optimal value of the dual objective function θ^D. In [27], it is suggested that other stable phases can be found by finding all solutions to the equation $G(\underline{x}, P^0, T^0) = G(\underline{x}^*, P^0, T^0) + \underline{\lambda}^{*T}(\underline{x}-\underline{x}^*)$, using algorithms such as those described in [55,56]. The equivalent formulation in the $(\underline{x}, V, T)$ space at pressure P^0 and temperature T^0 is

$$A(\underline{x},V,T^0)+P^0V=A(\underline{x}^*,V^*,T^0)+P^0V^*+\underline{\lambda}^{*T}(\underline{x}-\underline{x}^*). \quad (43)$$

The set of points $(\tilde{\underline{x}}, \tilde{V})$ that satisfy (43) is the set of all stable phases at the given conditions.

The property that all stable phases are global solutions of the dual problem can be used to propose an alternative approach. The knowledge of θ^D, the dual problem objective function value at the global solution, can be used to define the tangent plane that passes through all the stable phases:

$$\theta^D=A(\underline{x},V,T^0)+P^0V+\sum_{i=1}^{nc-1}\lambda_i^*(x_i^0-x_i). \quad (44)$$

By definition, θ^D is also the objective function value of the dual and of the inner problem $(IP_{x,V})$ at $\underline{\lambda}^*$. Thus, identifying all points that satisfy Eq. (44) is equivalent to finding all the global solutions of the inner problem where $\underline{\lambda}=\underline{\lambda}^*$:

$$\min_{\underline{x}\in X, V\in[\underline{V},\overline{V}]} A(\underline{x},V,T^0)+P^0V+\sum_{i=1}^{nc-1}\lambda_i^*(x_i^0-x_i). \quad (45)$$

Although finding all solutions of (43) or of (45) is equivalent, finding all (global) solutions of (45) can be achieved very efficiently as a final step of the solution of the dual problem $(D_{x,V})$, once $(\underline{x}^*, V^*, \underline{\lambda}^*)$ have been found. The practical aspects of such an implementation are discussed in the next section.

4. Algorithms for the solution of the phase equilibrium problem in the volume-composition space

Problem $(D_{x,V})$ is a bilevel programming problem that can be equivalently framed as a semi-infinite program (SIP):

$$\begin{aligned} \max_{v,\underline{\lambda}\in\mathbb{R}^{nc-1}} \quad & v \\ \text{s.t.} \quad & v \le A(\underline{x}, V, T^0) + P^0 V + \sum_{i=1}^{nc-1} \lambda_i (x_i^0 - x_i), \quad \forall \underline{x} \in X, V \in [\underline{V}, \overline{V}] \\ & v \le G^P \end{aligned} \tag{46}$$

A number of techniques have been developed to solve such problems [57–59]. Recent work on global optimisation approaches to the solution of SIP and bilevel problems is reviewed in [60], and there has been much recent progress on the solution of nonconvex bilevel problems ([61–64]). We present an algorithm to solve the volume-composition phase equilibrium problem by identifying all global solutions of problem $(D_{x,V})$, $(\underline{\lambda}^*, \underline{x}^{*,l}, V^{*,l})$, $l = 1, \ldots, np$, where np is the number of global solutions or phases (not known *a priori*). It is based on that presented in [27], following the general framework of Blankenship and Falk [57], but incorporates a number of modifications to find all stable phases and to enhance performance. The method is suitable for any EOS formulated in the $(\underline{x}, V, T)$ space. The only property required for the P, T flash calculation is a continuous Helmholtz free energy surface.

In the first stage of the algorithm, we focus on finding one of the global solutions of the problem, i.e., the unique vector $\underline{\lambda}^*$ which is common to all phases and a phase coordinate $(\underline{x}^{*,1}, V^{*,1})$. In the second stage, we use a post-processing step in order to find all other global solutions. The first stage of the algorithm is a cutting plane method [46,57]. It consists of two alternating steps; a linear maximisation in $\underline{\lambda}$, the outer problem, and a nonlinear minimisation in $(\underline{x}, V)$, the inner problem. When the solutions to these two problems converge to within an optimality tolerance ϵ, the algorithm is terminated. The outer problem is a linear approximation of the dual problem and it has the following form:

$$\begin{aligned} UBD^V \quad = & \max_{v,\underline{\lambda}\in\mathbb{R}^{nc-1}} v \\ \text{s.t.} \quad & v \le A(\underline{x}^m, V^m, T^0) + P^0 V^m + \sum_{i=1}^{nc-1} \lambda_i (x_i^0 - x_i^m), \quad \forall [\underline{x}^m, V^m] \in \mathcal{M} \\ & v \le G^P \end{aligned} \tag{$\mathrm{OP}_{x,V}$}$$

where UBD^V is an upper bound on θ^D, $\mathcal{M}$ is a set of points $(\underline{x}, V) \in X \times [\underline{V}, \overline{V}]$. The set $\mathcal{M}$ initially consists of a set of $2(nc-1)$ points. The solution of this outer problem yields a vector $\underline{\lambda}$, which is then used in the formulation of the inner problem $(\mathrm{IP}_{x,V})$. The solution of the inner problem provides a new coordinate $[\underline{x}, V]$ that can be added to set $\mathcal{M}$, thereby adding a new cutting plane to the outer problem. As will be discussed, in our approach, it is sometimes possible to generate more than one $[\underline{x}, V]$ point for a given value of $\underline{\lambda}$. The outer problem and inner problem also provide upper and lower bounds on the global solution of the dual problem. The algorithm iterates between the solution of the two problems until these bounds converge to within a specified tolerance.

We do not require the cutting planes generated by the solution of $(\mathrm{IP}_{x,V})$ to be tangential to the dual function although, in principle, non-tangential planes may increase the number of iterations required to solve the problem. The advantage of such an approach is that the cutting planes are obtained by performing a local optimisation, whereas a tangential approximation requires the application of a global optimisation algorithm. The cost of each new plane is thus significantly lower than in a tangential algorithm. Furthermore, in practice, good quality cutting planes tend to be identified by the local optimiser, especially if a few different starting points are used. Convergence of the proposed algorithm is guaranteed by using global optimisation when the results of the local optimisation indicate convergence has been achieved, or when the local optimisation fails to return a suitable solution. We also propose an alternative formulation of the inner problem which speeds up the global solution of the inner problem.

Before presenting the algorithm, we discuss the basic elements of the approach: the initialisation strategy, the implications of using a local solver for the inner problem, alternative formulations for the inner problem, the identification of all stable phases, and a strategy for dealing with small values of the mole fractions.

4.1. Problem initialisation

At the start of the algorithm, both an initial guess and bounds are required for $\underline{\lambda}$. The choice of values affects the performance of the algorithm by determining the initial upper and lower bounds on the global solution. With a view to algorithmic efficiency when the state of the system is unknown, we initialise $\underline{\lambda}$ to be the gradient of the Gibbs free energy surface at $\underline{x}^0$ i.e., $\lambda_i^0 = (\partial G/\partial x_i)_{x_i = x_i^0, P, T}$. This allows the first iteration to double as a stability test, whereby if the global solution of the first inner problem lies at G^P and $(\underline{x}^0, V^0)$, then the total composition corresponds to a stable phase. Furthermore, if there is only one global solution to the inner problem, the system is in a single phase at $(\underline{x}^0, P^0, T^0)$. If the feed is stable, but there are multiple global solutions, then the overall composition lies on a phase boundary. Other global solutions correspond to these stable phases.

Bounds for $\underline{\lambda}$ can be specified by selecting appropriate values of the composition (and volume) and using them to initialise the set $\mathcal{M}$, and hence the set of constraints in the outer problem $(\mathrm{OP}_{x,V})$. The bounding scheme for $\underline{\lambda}$ detailed in [27] is effective, except when the mole fraction of one component in the feed is very low, in which case wide bounds are obtained. We retain the notation of [27] where two composition vectors, $\underline{\bar{x}}^i$ and $\underline{\hat{x}}^i$, are chosen to bound each λ_i. $\underline{\bar{x}}^i$ has the property $\bar{x}_i^i > x_i^0$ and $\underline{\hat{x}}^i$ that $\hat{x}_i^i < x_i^0$. In [27], the $\underline{\hat{x}}$ and $\underline{\bar{x}}$ are such that the lower and upper bounds for a given λ_i depend inversely on $x_i^0 - \hat{x}_i$ and $x_i^0 - \bar{x}_i$. When those differences are small (i.e., when x_i^0 is very close to 0 or 1), the bound on λ_i becomes very loose. The scheme proposed here ensures that the bounds on λ_i depend on the entire $x_i^0 - \hat{x}_i$ and $x_i^0 - \bar{x}_i$ vectors. The modified bounding scheme retains the idea of choosing bounds to enclose $\underline{x}^0$, but ensures that the scheme remains effective when some components are present in small mole fractions. The simple bounding scheme that we have implemented takes values on either side of x_i^0, for a given component, i, and then assigns equal contributions to the rest of the initialisation vector. This is as follows:

$$\left.\begin{aligned} \hat{x}_i^i &= \frac{x_i^0}{2} \\ \hat{x}_k^i &= \frac{1 - \hat{x}_i^i}{nc-1}, \quad \text{for } k = 1, \ldots, nc-1, \quad k \ne i \\ \bar{x}_i^i &= \frac{1 + x_i^0}{2} \\ \bar{x}_k^i &= \frac{1 - \bar{x}_i^i}{nc-1}, \quad \text{for } k = 1, \ldots, nc-1, \quad k \ne i \end{aligned}\right\}, \quad \text{for } i = 1, \ldots, nc-1. \tag{47}$$

This produces a set of initial compositions $\mathcal{M}^0$, which lead to:

$$\begin{aligned} v &\leq A(\underline{\hat{x}}^i, \hat{V}^i, T^0) + P^0\hat{V}^i + \sum_{k=1}^{nc-1}\lambda_k(x_k^0 - \hat{x}_k^i) \\ v &\leq A(\underline{\bar{x}}^i, \bar{V}^i, T^0) + P^0\bar{V}^i + \sum_{k=1}^{nc-1}\lambda_k(x_k^0 - \bar{x}_k^i), \quad \text{for } i = 1, \ldots, nc-1. \end{aligned} \tag{48}$$

It can be shown that the set of inequalities in (48) provide lower and upper bounds on each λ_i. $\bar{V}^i$ and $\hat{V}^i$ can either be chosen to solve the pressure equation for a given $\underline{\bar{x}}^i$ or $\hat{x}^i$, respectively, or can simply take any feasible value ($V \in [\underline{V}, \bar{V}]$). However, the bounds provided by the volumes corresponding to the specified pressure P^0 are likely to be tighter. If we recall that solution of the pressure equation is a minimisation of free energy with volume ($\min_{V\in[\underline{V},\bar{V}]}[A(\underline{x}, V, T^0) + P^0V]$), then these bounds represent the lowest possible cutting planes on $\theta(\underline{\lambda})$ at $\underline{\bar{x}}^i$ or $\underline{\hat{x}}^i$.

To illustrate this procedure, we construct the bounding compositions for a ternary system. Consider the following feed composition,

$$\underline{x}^0 = \begin{pmatrix} 0.2 \\ 0.3 \\ 0.5 \end{pmatrix}. \tag{49}$$

The outer problem for such a feed composition is initialised with the following four points in composition:

$$\underline{\hat{x}}^1 = \begin{pmatrix} 0.10 \\ 0.45 \\ 0.45 \end{pmatrix}; \quad \underline{\bar{x}}^1 = \begin{pmatrix} 0.6 \\ 0.2 \\ 0.2 \end{pmatrix};$$

$$\underline{\hat{x}}^2 = \begin{pmatrix} 0.425 \\ 0.150 \\ 0.425 \end{pmatrix}; \quad \underline{\bar{x}}^2 = \begin{pmatrix} 0.175 \\ 0.650 \\ 0.175 \end{pmatrix}. \tag{50}$$

For each point in composition, we locate the volume root at the lowest Gibbs free energy for the fixed composition. These points in composition and volume are then used to initialise the set $\mathcal{M}$. It can be shown that the set of cutting planes thus generated provides upper and lower bounds on all components of the $\underline{\lambda}$ vector.

4.2. Use of local solutions to the inner problem

The inner problem plays two roles in the solution of the dual problem: for a given $\underline{\lambda}^k$, it is used to generate good quality cutting planes for the master problem, by identifying composition-volume points for which the Lagrange function $L^V(\underline{x}, V, \underline{\lambda}^k)$ is low; it is also used to generate a valid lower bound on the dual function and hence to allow a convergence test to be applied. Identifying a local solution $(\underline{x}^k, V^k)$ of the inner problem rather than the global solution $(\underline{x}^{k,*}, V^{k,*})$ is attractive as it is computationally less demanding. It has the following implications:

- A cutting plane

$$c(\underline{\lambda}) = A(\underline{x}^k, V^k, T^0) + P^0V^k + \sum_{i=1}^{nc-1}\lambda(x_i^0 - x_i^k) \tag{51}$$

resulting from a non-global solution is valid but is not tangential to the dual objective function. Thus, including this cut in the master problem rather than the cut corresponding to the global solution $(\underline{x}^{k,*}, V^{k,*})$ results in an approximation of the dual problem that is less tight, leading to a looser upper bound on the global solution θ^D than might have been obtained with a tangential plane. This concept is represented in Fig. 3. It implies that any coordinate of $[\underline{x} \in X, V \in [\underline{V}, \bar{V}]]$ is a valid upper bound on θ^D. The use of such a cutting plane may increase the number of iterations required to achieve convergence of the algorithm. In addition, it is possible for such a cutting plane to be redundant, so that solving the master problem with this new cut does not yield an improvement on the upper bound and, more importantly, does not yield a new vector $\underline{\lambda}$. In this case, it is essential to generate an improved cut for $\underline{\lambda}^k$. This can be done by solving the inner problem to global optimality. In practice, it is not necessary to identify a global solution of the inner problem: a point with a lower objective function than $(\underline{x}^k, V^k)$ may suffice.[3]

- The value of the objective function of the inner problem obtained by using a local solver is not necessarily a valid lower bound on the global solution of the problem. This implies that this value cannot be used to determine conclusively whether convergence has been achieved. It is stored as a tentative lower bound. When the difference between the global upper bound and the highest tentative lower bound is within the convergence tolerance, the inner problem must be solved globally. The resulting global lower bound then indicates whether convergence has indeed been achieved, i.e., the local solution of the inner problem is in fact its global solution. If not, the upper bounding problem is then solved again to provide a new guess for $\underline{\lambda}$. In cases where a non-global solution to the inner problem is found by the local solver, it is possible for the tentative lower bound to be greater than the global upper bound. In this instance, a better solution to the inner problem must be sought. This can be done by solving the inner problem to global optimality or running a global solver until it identifies a better solution.

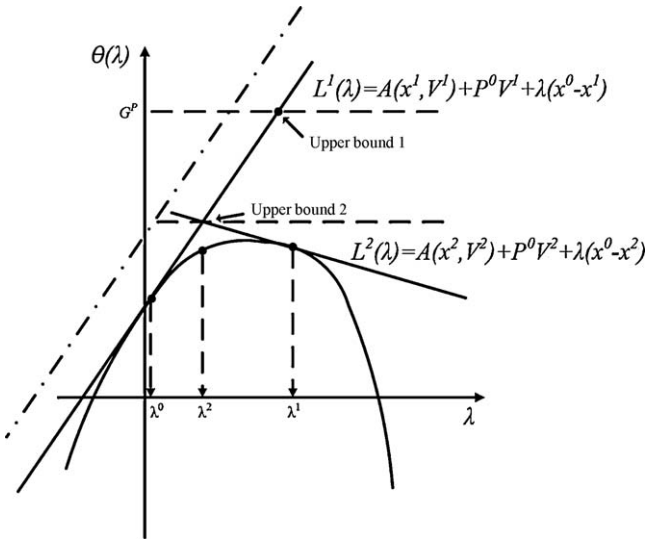

Fig. 3. A schematic representation of the concave dual objective function $\theta(\lambda)$ and the cutting/tangent planes used to provide a monotonically decreasing upper bound on the solution of the dual problem, in a binary system. Note that the curvature of the dual function is exaggerated for visual clarity. The state of the dual problem after two min/max cycles (after iteration 2) is shown here. At the first iteration, $\lambda^{(0)}$ is g^0, the gradient of the Gibbs free energy surface at x^0. L^1, the tangent to the $\theta(\lambda)$ curve at $\lambda^{(0)}$ is the tangent plane given by the global solution of the inner problem for $\lambda^{(0)}$. The solution of the outer problem for the first time, bounded by this plane and G^P, does not reduce the value of the upper bound ($UBD^1 = G^P$), but does furnish a new value for the Lagrange multiplier, $\lambda^{(1)}$. The inner problem is solved for $\lambda^{(1)}$, providing a second tangent plane, L^2. The solution of the outer problem with the additional bound that this provides leads to a reduction in the value of the upper bound i.e., $UBD^1 > UBD^2$. The dot-dash line is a cutting plane obtained from a non-global solution of the inner problem for $\lambda^{(0)}$. If this were used in the outer problem instead of the tangential plane for $\lambda^{(0)}$, a different value of $\lambda^{(1)}$ would be obtained.

[3] In the implementation discussed here, we solve the inner problem to global optimality in such cases.

4.3. Alternative formulations of the inner problem

The inner problem ($IP_{x,V}$) is a bound-constrained nonlinear problem. In deterministic global optimisation algorithms, improvements in computational performance may be achieved by adding redundant constraints, that do not change the solution of the problem, but that may affect the performance of the global solver by allowing tighter relaxations of the nonconvex problem to be constructed [65–68]. These added constraints can reduce the size of the feasible region of the convex relaxation significantly, and hence lead to much better lower bounds. In the case of a problem with only linear constraints such as ($IP_{x,V}$), the only redundant constraints that may be added are the first-order optimality conditions, Eqs. (29) and (30). In our experience, explicit inclusion of the pressure constraint (29) greatly reduces the number of nodes explored by spatial branch-and-bound (sBB) global optimisation algorithms, such as BARON [51,52] and αBB[4][53,54,69], during the solution of the inner problem. This usually leads to improvements in computational time, although this is dependent upon the additional computational load incurred by the inclusion of these constraints in the optimisation problem. The inclusion of the chemical potential constraints (30) does not consistently improve computational performance and is therefore not recommended. The following inner problem formulation for a given $\underline{\lambda}^k$ is then used when a deterministic global optimisation algorithm is applied:

$$\begin{aligned} \min_{\underline{x}\in X, V\in[\underline{V},\overline{V}]} \quad & L^V(\underline{x}, V; \underline{\lambda}^k) \\ \text{s.t.} \quad & -\left(\frac{\partial A(\underline{x}, V, T^0)}{\partial V}\right)_{\underline{x},T} = P^0. \end{aligned} \qquad (IP^{global}_{x,V})$$

One of the features of the formulation in the $\underline{x}$–V space is that it is not necessary to solve the pressure equation explicitly and the introduction of (29) in the formulation of the inner problem at first seems to negate this. It should however be noted that the pressure equation is not solved at every evaluation of the objective function, as is the case in the composition space. In the inner problem of the sBB algorithm, a convex relaxation of the pressure equation is included, which requires simple evaluations at each iteration rather than the use of a nonlinear solver. It is not necessary to include the pressure equation in the outer problem for the sBB algorithm, but it is advantageous to do so from the point of view of implementation, provided that an infeasible path local solver is used. The inclusion of the constraint ensures that the accuracy with which the pressure at the solution of the outer problem matches P^0 is high. This is because this constraint can then be enforced through a feasibility tolerance that is tighter than the optimality tolerance.

4.4. Finding all stable phases

All stable phases present at equilibrium are solutions to the dual problem. Therefore, when the algorithm has converged to the equilibrium value of $\underline{\lambda}$, each stable phase is a global solution to the inner problem ($IP_{x,V}$) or, equivalently, ($IP^{global}_{x,V}$). If a spatial branch-and-bound algorithm is used to solve the inner problem, it is not able to discard or fathom any of the nodes containing the stable phases, since all these solutions are equally good (see [50] or [70] for a discussion of spatial branch-and-bound methods). Depending on the implementation used, the sBB algorithm either explores the branch-and-bound tree until the list of lower bounds is empty, in which case it must report all global solutions, or, as is more often the case, it terminates once the upper and lower bound have converged to within the optimality tolerance. In such implementations, when the sBB algorithm reports one solution, there are other nodes in its list of lower bounds that are of equivalent quality (within ϵ, the optimality tolerance). However, global optimisation algorithms are not generally set up to return all solutions. In particular, while there may be several nodes with equivalent lower bounds, one needs to ascertain how many global solutions (none, one or more) lie in each of the regions of the variable space defined by these nodes. Thus, some post-processing is necessary on the final list of nodes. Each node that remains in the list once the first global solution has been found must be analysed and convergence can only be achieved once all the regions in the list are smaller than a given size (e.g., using the infinity norm) *and* have been shown to contain a solution to ($IP^{global}_{x,V}$). The solutions to ($IP^{global}_{x,V}$) remaining in the list at this stage can be reported as the stable phases.

4.5. Dealing with small mole fractions

When searching for solutions of the phase equilibrium problem with a guaranteed deterministic approach, it is usually necessary to bound the mole fractions by a small but finite number, e.g. 10^{-16}, to avoid numerical difficulties arising from the evaluation of $\log x$ at small mole fractions (e.g. [18]). Phases containing at least one component in very small amounts are often encountered when dealing with polymer-solvent mixtures. The range of mole fractions accessible for exploration can be extended by formulating the problem in terms of logarithms of mole fractions, or in terms of logarithms of mass fractions. This can, however, lead to slow convergence of the algorithm as large regions of very small mole fractions typically need to be explored by the branch-and-bound algorithm. A reliable, if not guaranteed, way to deal with this issue is to use a larger lower bound on the mole fractions, such as 10^{-8} and to adjust the convergence tolerance to avoid eliminating phases prematurely, e.g. 10^{-5}: if the true mole fraction of a phase is below the chosen lower bound, an approximate solution will be found at the bound within an appropriate convergence tolerance. If such a solution is identified, its accuracy can then be increased by solving locally a two-dimensional constrained problem in the mole fraction be to refined, and in volume (where the search is in the logarithm of both variables). This constrained problem is formulated to find a mole fraction satisfying the optimality criteria on the specified pressure and the equilibrium chemical potential:

$$\begin{aligned} \min_{x_{k,j}\in\hat{X}, V_j\in[\underline{V},\overline{V}]} \quad & (\mu_{k,j}(x_{k,j}, V_j) - \mu_k^*)^2, \\ \text{s.t.} \quad & P_j(x_{k,j}, V_j) = P^0. \end{aligned} \qquad (52)$$

where $x_{k,j}$ is the mole fraction in phase j, to be refined, $\hat{X}$ is the modified search area corresponding to a smaller lower bound (e.g., 10^{-50}), $\mu_{k,j}$ is the chemical potential of the trace component k in phase j and μ_k^* is the equilibrium chemical potential of component k (related to the optimal value of the Lagrange multiplier, λ_k^*). P_j is the pressure of phase j and P^0 the pressure specified for the flash calculation. The lower bound on the mole fraction being explored can be set to a very small value, since the use of logarithmic space reduces the numerical difficulties associated with setting very low bounds on $\underline{x}$. Alternatively, the approach proposed by Lucia et al. [15] can be used to refine the phase composition.

4.6. The phase equilibrium algorithm

The proposed algorithm is summarised in Table 1 as a procedure and in Fig. 4 as a flowchart. In subsequent discussions, we will refer to this algorithm as the 'Local + Global' approach. In the first step of the algorithm, variables are initialised. This includes the iteration counter, k, the upper bound UBD, which is set equal to the Gibbs

[4] The α BB implementation of the algorithm will be described in a subsequent publication.

Table 1
Proposed algorithm for the solution of the phase equilibrium problem.

PROCEDURE Solve Phase Equilibrium($\underline{x}^0$, P^0, V^0)
Step 1 – Initialisation
(a) Set iteration counter $k=0$;
Upper bound UBD=$G(\underline{x}^0, P^0, V^0)$;
Lower bound LBD=$-\infty$;
Set of local lower bounds $\mathcal{L}=\varnothing$.
(b) Set $\lambda_i^{(0)} = \left(\frac{\partial G}{\partial x_i}\right)_{x_i=x_i^0,P,T} = g_i^0$
(c) Initialise set $\mathcal{M}$ based on Eq. (47).
Step 2 – Generation of a cutting plane
Solve the inner problem ($IP_{x,V}$) locally N_{local} times at fixed $\underline{\lambda}^k$.
If a solution has been found:
Add lowest solution $L^{V,(k)}$ to $\mathcal{L}$.
Add the corresponding variable values ($\underline{x}^{(k)}$, $V^{(k)}$) to $\mathcal{M}$.
Else, go to Step 5.
Step 3 – Test need for global optimisation
If UBD $-L^{V,(k)} \le \epsilon$, go to Step 5.
Step 4 – Solve the outer problem ($OP_{x,V}$)
If the solution $\underline{\lambda}^*$ is such that $|\lambda_i^* - \lambda_i^{(k)}| \le \epsilon_n$, $i=1,\ldots,nc-1$, go to Step 5;
Else set $\underline{\lambda}^{(k+1)} = \underline{\lambda}^*$ and go to Step 7.
Step 5 – Generation of a tangent plane
Find a global solution $L^{V,*}$ of the inner problem ($IP^{global}_{x,V}$) at fixed $\underline{\lambda}^k$.
If $L^{V,*}$ > LBD, set LBD = $L^{V,*}$ and add ($\underline{x}^{(k)}$, $V^{(k)}$) in $\mathcal{M}$ by the solution.
Step 6 – Test for overall convergence
If | UBD − LBD |$\le\epsilon$, a stable phase ($\underline{x}^{(k)}$, $V^{(k)}$, $\underline{\lambda}^{(k)}$) has been found. Go to Step 8.
Step 7 – Increment iteration counter $k=k+1$ and go to Step 2.
Step 8 – Find all stable phases
Identify and report all global solutions of the inner problem.
END Solve Phase Equilibrium;

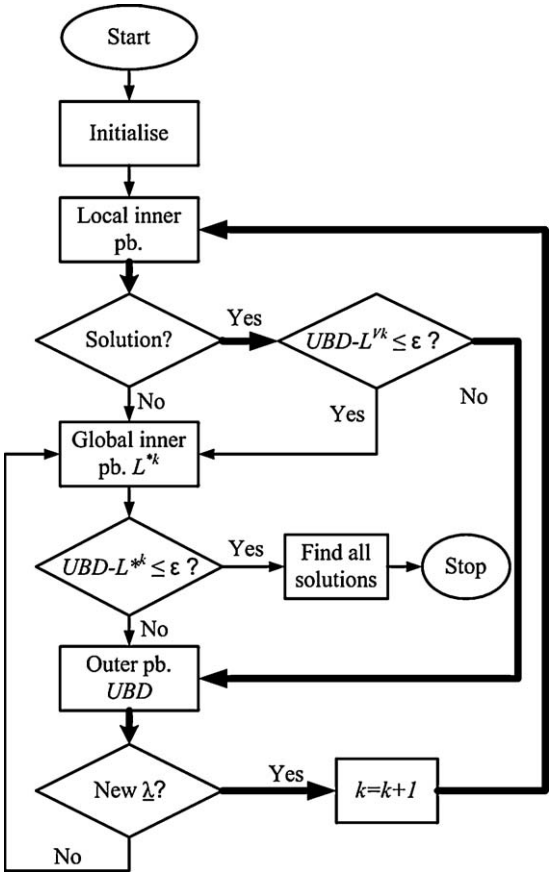

Fig. 4. Flowchart of the Local + Global algorithm for the global solution of dual problem ($D_{x,V}$).

free energy at the total composition (following computation of the stable volume root), the lower bound LBD, which is set to $-\infty$, an empty list of tentative lower bounds $\mathcal{L}$, the vector of Lagrange multipliers, $\underline{\lambda}^{(0)}$, which is set to g_0, the partial derivatives of G with respect to $\underline{x}$ at the total composition, and the set of cutting plane points $\mathcal{M}$.

In the second step, a cutting plane is obtained by solving the inner problem ($IP_{x,V}$) locally several (N_{local}) times from different starting points and retaining the best (lowest) solution. The objective function value at the solution is added to the set $\mathcal{L}$ and the corresponding variable values to $\mathcal{M}$. If no solution is found, the algorithm proceeds to Step 5, where the modified inner problem ($IP^{global}_{x,V}$) is solved globally. If a solution to the inner problem has been found, a test is applied in Step 3 to determine whether the inner problem needs to be solved globally.

The test in Step 3 is passed when the upper bound and the local lower bound are within a specified tolerance, indicating that the algorithm may have identified the global solution. It is also passed when the tentative lower bound is greater than the upper bound, indicating that the global solution of the inner problem has not been found by the local solver. In both cases, the algorithm proceeds to Step 5 to identify a guaranteed lower bound by solving the inner problem globally. If the test in step 3 fails, this indicates that the local solution of the inner problem has generated a cutting plane that can be added to the outer problem.

The outer problem ($OP_{x,V}$) is then formulated in Step 4 using all points in $\mathcal{M}$ and solved. The solution of this outer problem ($UBD^{V,k}$) is taken as the new upper bound on the solution of the dual. This maximisation step also results in a vector of Lagrange multipliers, $\underline{\lambda}^k$. If a different $\underline{\lambda}$ vector is found as the solution to the problem from that at the previous iteration, this vector is guaranteed to be closer to the global solution of the dual problem. In this case, a major iteration has been completed and the algorithm proceeds to Step 7 where the iteration counter is incremented. The algorithm then returns to Step 2 where the inner problem is solved locally.

If the solution of the outer problem does not result in a new $\underline{\lambda}$, the last cutting plane was too loose and a tangent plane is generated to replace it. This is done by proceeding to Step 5 and solving the inner problem to global optimality. This step is crucial as it guarantees the finite convergence of the algorithm to ϵ-optimality. There are thus three instances when the global optimisation of the inner problem is necessary. These can be seen most clearly in Fig. 4: (i) when the local solver fails to find a solution to the inner problem; (ii) when the local solver returns a solution that indicates convergence or that is greater than the upper bound; (iii) when the local solution of the inner problem generates a cutting plane that does not add any information to the outer problem. When Step 5 is carried out, a tangential plane and a valid lower bound on the dual solution are obtained. If the lower bound is greater than the current lower bound LBD, LBD is updated. Convergence is then tested in Step 6. If the test is satisfied, all the global solutions of the inner problem solved in Step 5 are identified and reported as stable phases.

The use of cutting planes and tangent planes is illustrated in Fig. 3. As can be seen in Fig. 4, the global solution of the inner problem lies at the heart of the algorithm. Convergence can only be reached if the global solution of the inner problem is obtained at least once. In practice, the need for global optimisation usually arises only at the final iteration, in which convergence is proved with a mathematical guarantee. The use of multiple random start local minimisations means that the global minimum of the inner problem is identified frequently enough so as not to impact significantly on the final iteration count. The route followed by the algorithm at other major iterations is highlighted by the thick black lines in Fig. 4.

4.7. Other algorithms for the solution of the phase stability problem in the volume-composition space

The algorithm of [27] can be used to solve the phase stability problem in the volume-composition space. The outer problem is given by ($OP_{x,V}$) and the inner problem by ($IP_{x,V}$). The inner problem is solved to global optimality at each iteration. We have implemented this algorithm in the volume-composition space, replacing the initialisation strategy of [27] with that described in Section 4.1 and including a final post-processing step to find all phases. We refer to this approach as the "Global" algorithm.

This algorithm can be extended to use the alternative formulation of the inner problem, ($IP^{global}_{x,V}$). We have also tested this option, to study the impact of the additional constraint on the performance of the global optimisation solver. We refer to this approach as "Global + Constraint".

5. Computational results

In order to assess the proposed formulation and the Local + Global algorithm, we carry out P, T flash calculations for a number of different systems. To illustrate the general concept, we begin by applying this method to solve for VLE, LLE and VLLE in hypothetical systems, modelled with an augmented van der Waals EOS [71–74]. A reliable algorithm for solving phase equilibrium in these systems, where the molecules are of equal size, has been developed by Giovanoglou et al. [2,3]. This allows us to assess the adequacy of our method on both two- and three-phase systems. We then proceed to calculations for highly asymmetric systems that exhibit the behaviour characteristic of solvent + polymer mixtures, modelled with the SAFT-HS (statistical associating fluid theory for a hard sphere reference) EOS [75]. Solvent–polymer systems exhibit highly non-ideal phase behaviour, and present a difficult challenge to any phase equilibrium solution method. In particular, the quantity of polymer in one of the phases is often very small, which can lead to numerical problems in phase equilibrium calculations. In addition, for polymer chain lengths of greater than six times that of the solvent, type V phase behaviour (according to the classification of Scott and van Konynenberg [76]) may be observed with a SAFT-like description [77]. This includes LLE at some conditions, bounded by a VLLE three-phase line and a lower critical solution temperature (LCST). This region in particular can lead to failure in some flash algorithms. Again, these systems exhibit both two- and three-phase regions, therefore an algorithm that does not require the *a priori* specification of the number of phases present at equilibrium is beneficial.

Following the presentation of the method for binary systems, we investigate the performance of the algorithm for ternary solvent + polymer mixtures with SAFT-HS model systems that exhibit VLE, LLE and LLLE. A method guaranteeing global stability is important with such highly non-ideal systems. Any reliance on initial guesses from nearly ideal systems, for example, could result in convergence problems, since such starting values may be far away from the true behaviour. In addition, the need for initial guesses in volume can create problems when moving between regions of VLE and LLE, since there is a discontinuity in the phase volumes when moving between these regions.

For each mixture, we use the three algorithms discussed in Section 4, comparing the results of the "Global" and "Global + Constraint" approaches to examine the impact of adding the optimality condition on pressure as a constraint in the inner problem, and comparing the results of the "Global + Constraint" and "Local + Global" approaches to quantify the impact of solving the inner problem with local methods. We show point calculations at fixed ($\underline{x}^0$, P^0, T^0) and also include the P–x or T–x phase diagrams for the binaries, and triangular phase diagrams at fixed T^0, P^0 for the ternaries, to demonstrate the consistency of the results over different systems and phase configurations.

5.1. Implementation

The three algorithms described in Section 4 have been implemented in GAMS 23.2 [78], using BARON V8.1.5 [52] for global optimisation, MINOS 5.51 [79] as the nonlinear local solver, and CPLEX 12.1.0 [80] for linear problems. Throughout, the different EOSs used have been implemented in packing fraction and composition space, since these variables are well bounded and many of the expressions in the EOS used as numerical examples can most naturally be formulated in packing fraction. Although the presentation of the dual problem in previous sections was in the more 'intuitive' space of volume, a proof that working either in packing fraction or volume produces equivalent results is presented in Appendix A.

One difficulty in implementing the phase equilibrium algorithm is that, though BARON can return multiple solutions of the inner problem, it is not set up to return only global solutions. We have found that the most effective way to identify all other phases is with a final 'multi-solution' iteration, after convergence of the dual. Thus, the inner problem for the optimal $\underline{\lambda}^*$ vector is solved a second time. Throughout the calculations in this article we select the BARON option to return three solutions during the final iteration for a binary and four for a ternary, with a minimum separation between these solutions of 10^{-4}. One may subsequently examine these solutions to ascertain how many phases or global solutions are present.

The absolute optimality tolerance used for the dual (stability) problem is $\epsilon = 10^{-7}$. The optimality tolerance for BARON, MINOS and CPLEX is $\epsilon = 10^{-8}$. In all problems, we set $X = [10^{-8}, 1]$, and use the approach described in Section 4.5 to identify components present in mole fractions smaller than 10^{-8}. As will be shown, we use packing fraction η instead of volume V and set initial bounds on η to $[10^{-6}, 0.73]$. The latter value corresponds to the close-packing limit of hard spheres, well above the fluid/solid packing fractions observed in real systems. A value of $N_{local} = 2$, 5 or 15 is used for the Local + Global runs, as indicated. The calculations are carried out on an HP Workstation (Intel Xenon, 3 GHz).

5.2. Calculations with an augmented van der Waals EOS

To demonstrate the reliability of the method and its implementation, we begin by comparing our results to the work of Giovanoglou et al. [2,3] who developed a reliable deterministic scheme for the solution of phase equilibria with an augmented van der Waals (AVDW) EOS [71–74], for binary mixtures of spherical, equal sized components. The spheres are assumed to have a volume (b) set equal to 1 for convenience, therefore packing fraction (η) and density (ρ) are equivalent, $\eta = \rho$. In this approach, the Helmholtz free energy of such a binary mixture is given by:

$$\frac{A}{NkT} = \sum_{i=1}^{2} x_i \ln(x_i \eta) - 1 + \frac{4\eta - 3\eta^2}{(1-\eta)^2} - \frac{\eta}{T'} \sum_{i=1}^{2} \sum_{j=1}^{2} x_i x_j \frac{\alpha_{i,j}}{\alpha_{2,2}}, \qquad (53)$$

where $\alpha_{i,j}$ is the van der Waals attractive constant.

The phase equilibrium calculations are conducted at constant temperature, therefore the purely temperature dependent (kinetic) terms have been excluded from the ideal part of Eq. (53). The corresponding Gibbs free energy (where the pressure features as a constant, P^0) is therefore given by:

$$\frac{G}{NkT} = \frac{A}{NkT} + \frac{P^0V}{NkT} = \sum_{i=1}^{2} x_i \ln(x_i\eta) - 1 + \frac{4\eta - 3\eta^2}{(1-\eta)^2} - \frac{\eta}{T'}\sum_{i=1}^{2}\sum_{j=1}^{2} x_i x_j \frac{\alpha_{i,j}}{\alpha_{2,2}} + \frac{P'}{T'\eta}. \quad (54)$$

The temperature and pressure are scaled by the attractive constant of the second component, and are described in terms of the reduced units T' and P':

$$T' = \frac{kTb}{\alpha_{2,2}}, \quad (55)$$

$$P' = \frac{P^0b^2}{\alpha_{2,2}}. \quad (56)$$

By writing the free energy in this reduced form only two parameters are required to describe the attractive interactions of the binary mixture, $\alpha_{1,1}/\alpha_{2,2}$ and $\alpha_{1,2}/\alpha_{2,2}$. One may observe from Eq. (54) that this EOS is a higher-than-cubic function in volume, a property of most complex EOSs.

We present calculations for two of the model systems studied by Giovanoglou et al. [3]. System A has a fluid phase equilibria of type I according to the classification of van Konynenburg and Scott [76], indicating that the only phase equilibria occurring at any conditions within the fluid range are vapour–liquid (VLE), and that this system forms a maximum of two phases at equilibrium. For example, a binary mixture of methane and carbon dioxide exhibits this type of phase behaviour. System B displays type II phase behaviour [3,76], which is characterised by the liquid phase demixing at low temperatures (below the upper-critical solution temperature, UCST). At low pressures, a three-phase line terminating at an upper-critical end point is observed. Real systems exhibiting this kind of phase behaviour include mixtures of alkanes and perfluoroalkanes, and mixtures of CO_2 and alkanes of intermediate chain length (i.e., C_8–C_{12}) [81]. We will use this system to demonstrate the ability of the new method to predict accurately the number of phases present at equilibrium, by carrying out a calculation in the region of the three-phase line.

For both systems, we have tested the consistency of the approach around all areas of the phase diagram, especially in challenging regions such as the vicinity of three-phase lines, where there may exist very small regions of two-phase separation, and also near critical points. We have carried out many thousands of calculations over a wide range of conditions, for the two systems highlighted and for others not included here. We report the first calculation in more detail to provide some insight into the proposed approach. All calculations are carried out with the 'full' Gibbs free energy, as opposed to the Gibbs free energy of mixing, where the free energy of the pure components is subtracted from the total free energy [81]. However, the free energy of mixing ΔG^{mix} is plotted where the Gibbs free energy-composition functions are shown for illustrative purposes, since the curvature of the surface is more pronounced and clearer to visualise. To obtain the ΔG^{mix} plots, we first obtain the Gibbs free energy at the most stable volume root for each of the pure components. We then step in composition, minimising the Gibbs free energy with volume at each fixed composition, to obtain a function at specified pressure and temperature. Finally we subtract the pure component Gibbs free energies, weighted by the mixture composition at the point of interest, to produce ΔG^{mix}.

5.2.1. System A: VLE with the AVDW EOS

We begin with an example of VLE in a type I mixture, as defined by the classification of van Konynenburg and Scott [76]. Attractive constants of $\alpha_{1,1}/\alpha_{2,2} = 0.5$ and $\alpha_{1,2}/\alpha_{2,2} = 0.8$ are examined [3] and correspond to a type I mixture. We carry out a flash calculation at $T' = 0.061295$, $P' = 3 \times 10^{-3}$ and $x_1^0 = 0.7$ using the Local + Global algorithm. To clarify the algorithmic steps as far as possible, we illustrate the progression of the algorithm through the major iterations. This is presented in Table 2. The only major iteration that requires the solution of the inner problem to global optimality is the final iteration. The purely global algorithms (Global or Global + Constraint) converge in the same number of major iterations. The stable phase compositions identified are shown in Table 3. There are two phases present at equilibrium for this combination of (x^0, P', T'), one liquid and one vapour with compositions and densities corresponding to the results of [3]. The P'–x_1 diagram for this system at $T' = 0.061295$, obtained though a series of independent calculations, is shown in Fig. 5(a). Again, this is in agreement with the work of [3].

Table 2
Iterations of Local + Global algorithm to identify the stable phases present in system A (VLE for a binary system with an AVDW EOS) at $T' = 0.061295$, $P' = 3 \times 10^{-3}$ and $x_1^0 = 0.7$. $G^p = -4.1034263054$ and λ^0 (gradient at x^0)=2.7229698414. The only major iteration for which a global solution of the inner problem is required is indicated by *. The order of calculations at each iteration is as follows: (1) solution of the minimisation ($IP_{x,V}$) at fixed λ to obtain a (local) lower bound, a new x_1 and a new η; (2) solution of the maximisation ($OP_{x,V}$) using all values of x_1 found so far to obtain an upper bound and a new λ. The stopping criterion is convergence of the outer and inner problems of $(UBD^j - LBD^j) < 1 \times 10^{-7}$.

Iteration	*UB*	*LB*	λ	x_1	η
1	−4.10343	−4.16237	2.40547	0.88564	0.07179
2	−4.12448	−4.14823	2.51889	0.49061	0.30062
3	−4.12588	−4.12695	2.51221	0.86053	0.07491
4	−4.12694	−4.12806	2.51884	0.53230	0.28839
5	−4.12695	−4.12695	2.51887	0.53509	0.28751
6*	−4.12695	−4.12695	2.51887	0.53510	0.28751

To give an idea of the functions involved in these phase equilibrium calculations, the Gibbs free energy of mixing (ΔG^{mix}) plotted against the mole fraction of component 1 (x_1) is shown in Fig. 5(b). The compositions of the stable phases are indicated by filled circles. We also show the function $\theta(\underline{\lambda})$ (c), and the set $\mathcal{G}$ (d), for this case study.

5.2.2. System B: VLLE with the AVDW EOS

This system exhibits type II fluid phase behaviour, and was also examined in [3]. It is modelled with the AVDW EOS, now with attractive constants of $\alpha_{1,1}/\alpha_{2,2} = 0.5$ and $\alpha_{1,2}/\alpha_{2,2} = 0.69$. To demonstrate the ability of the method to predict correctly the number of phases present we perform a flash calculation at conditions corresponding to the three-phase line, $T' = 0.051865$ and $P' = 0.0024981$. The procedure in this calculation is exactly the same as for the example with system A, though there are now three phases in coexistence. The Local + Global algorithm identifies the optimal $\underline{\lambda}^*$ vector after 4 iterations, though the global optimisation routine is called twice during the procedure. The properties of the three stable phases at the specified pressure and temperature are displayed in Table 4. Once again, they are in agreement with the work of Giovanoglou et al. [3]. The P'–x_1 diagram for this system, obtained though a series of calculations for different (x_1^0, P') combinations, is shown in Fig. 6(a). A plot of ΔG^{mix} against the mole fraction of component 1 is also shown in Fig. 6(b), along with of the location of the three stable phases. The generality of this method is particularly useful for phase diagrams such as that shown in Fig. 6(a),

Table 3
The stable phases for system A (VLE for a binary system with an AVDW EOS) at $T' = 0.061295$, $P' = 3 \times 10^{-3}$ and $x_1^0 = 0.7$.

	Phase I	Phase II
x_1	0.8605	0.5351
η	0.0749	0.2875

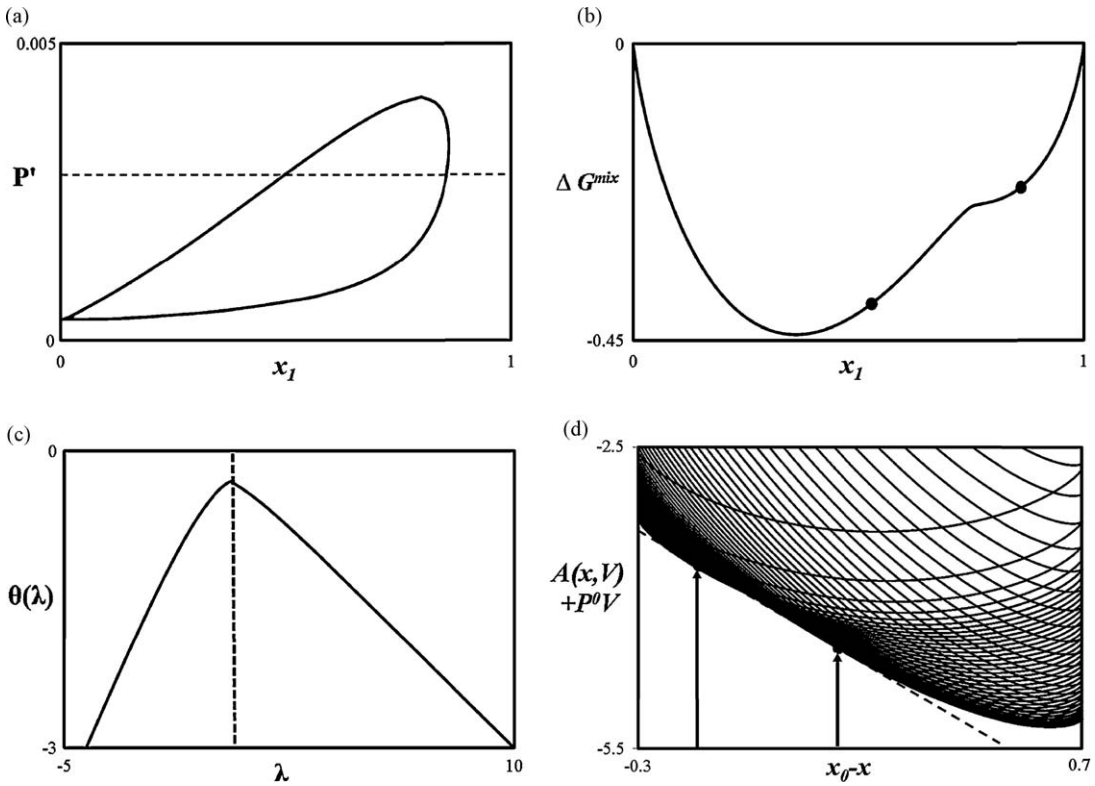

Fig. 5. System A (VLE for a binary system with an AVDW EOS). (a) P'–x_1 diagram at $T' = 0.061295$. The continuous curve corresponds to the phase boundary and the dashed line to $P' = 0.003$. x_1 is the mole fraction of component 1 in the mixture. (b) The Gibbs free energy of mixing at $T' = 0.061295$ and $P' = 0.003$. The filled circles are the stable equilibrium phases present at these conditions. (c) The dual objective function $\theta(\lambda)$ at $T' = 0.061295$ and $P' = 0.003$. The maximal value of $\theta(\lambda)$ lies at the λ corresponding to the equilibrium chemical potential, indicated by the vertical dashed line. (d) The set $\mathcal{G}$ at $T' = 0.061295$ and $P' = 0.003$. This corresponds to the example shown in Fig. 1. The lower boundary is the Gibbs free energy surface, $G(\underline{x}, P^0, T^0)$. The dashed line is the supporting tangent plane at the solution of the dual. The stable equilibrium phases, are indicated by the vertical arrows.

Table 4
Stable phases for system B (VLLE for a binary system for an AVDW EOS) at $T' = 0.051865$ and $P' = 0.00249810$. $x_1^0 = 0.5$.

	Phase I	Phase II	Phase III
x_1	0.6138	0.4703	0.9281
η	0.3035	0.3425	0.0878

where there may be VLE or LLE, depending on the global composition. No initial guesses are required, neither in terms of the number of phases, nor in terms of their compositions and volumes, meaning that no assumptions are made as to whether a phase is liquid or vapour.

5.3. Binary systems modelled with the SAFT-HS EOS

We now consider examples of phase equilibrium calculations in model polymer + solvent systems. This phase behaviour is more challenging from a numerical perspective since the phase splits may be very extreme, often including at least one essentially-pure phase. The SAFT-HS EOS [75,82–85] is implemented for these examples. The dispersion interactions are treated at the van der Waals mean-field level and calculations are restricted to mixtures of non-associating chain molecules. This EOS allows the entire range of fluid phase behaviour, except type VI [86], to be reproduced, providing a wealth of challenging test cases. In our case studies, all segments are taken to be of the same size and interact with the same

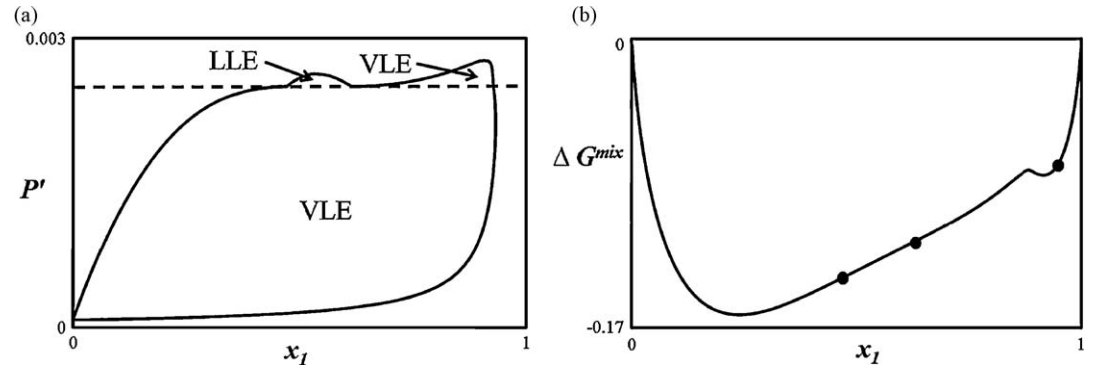

Fig. 6. System B (VLLE for a binary system for an AVDW EOS). (a) P'–x_1 diagram at $T' = 0.051865$. The continuous curve corresponds to the phase boundary and the dashed line to the three-phase pressure of $P' = 0.0024981$. (b) The Gibbs free energy of mixing at $T' = 0.051865$ and $P' = 0.0024981$. The filled circles are the stable equilibrium phases present at these conditions. x_1 is the mole fraction of component 1 in the mixture.

attractive energy, i.e., $\alpha_{11} = \alpha_{22} = \alpha_{12}$, ..., etc. This means that the only difference between molecules is their chain length. The binary mixtures are modelled as containing one component consisting of a single, spherical segment ($m_1 = 1$) of diameter σ and a second component consisting of m_2 tangentially bonded spherical segments ($m_2 > 1$) also of diameter σ. As with the AVDW EOS, the calculations are carried out at reduced temperatures and pressures. The simplified version of the SAFT-HS EOS that we implement in this work is essentially the AVDW EOS with the addition of a contribution to the free energy from the formation of a chain of tangentially bonded spherical segments. The Helmholtz free energy A of a molecule may be written as the sum of ideal (A^{IDEAL}), hard sphere (A^{HS}), mean field (A^{MF}) and chain (A^{CHAIN}) terms:

$$\frac{A}{NkT} = \frac{A^{IDEAL}}{NkT} + \frac{A^{HS}}{NkT} + \frac{A^{MF}}{NkT} + \frac{A^{CHAIN}}{NkT}. \tag{57}$$

In a mixture of nc components, all constructed from segments of diameter σ, the chain term is as follows:

$$\frac{A^{CHAIN}}{NkT} = -\sum_{i=1}^{nc} x_i(m_i - 1)\ln[g^{HS}(\sigma)], \tag{58}$$

where the Carnahan and Starling EOS [87] is used to give an expression for the contact value of the hard-sphere pair correlation function [83]

$$g^{HS}(\sigma) = \frac{1 - \eta/2}{(1-\eta)^3}. \tag{59}$$

The packing fraction is no longer equivalent to density, since the chain molecules contain more than one spherical segment. The relationship between packing fraction and density is now

$$\eta = \rho \sum_{i=1}^{nc} x_i m_i. \tag{60}$$

Since the dispersive energies of the molecules are modelled as identical ($\alpha = \alpha_{11} = \alpha_{12} = \alpha_{22}$, etc.), the mean-field term reduces to

$$\frac{A^{MF}}{NkT} = -\frac{\rho}{kT}\alpha\left(\sum_{i=1}^{nc} x_i m_i\right)^2 = -\frac{\eta}{T'}\left(\sum_{i=1}^{nc} x_i m_i\right). \tag{61}$$

The total Helmholtz free energy of a multi-component system modelled with the SAFT-HS EOS, where the attractive interactions of all components are identical is therefore

$$\frac{A}{NkT} = \sum_{i=1}^{nc} x_i \ln(x_i\rho) - 1 + \sum_{i=1}^{nc} x_i m_i \frac{4\eta - 3\eta^2}{(1-\eta)^2} - \frac{\eta}{T'}\left(\sum_{i=1}^{nc} x_i m_i\right) - \sum_{i=1}^{nc} x_i(m_i - 1)\ln[g^{HS}(\sigma)]. \tag{62}$$

As with the AVDW EOS, to obtain the Gibbs free energy we add a 'PV' term to Eq. (62), giving:

$$\frac{G}{NkT} = \sum_{i=1}^{nc} x_i \ln(x_i\rho) - 1 + \sum_{i=1}^{nc} x_i m_i \frac{4\eta - 3\eta^2}{(1-\eta)^2} - \frac{\eta}{T'}\left(\sum_{i=1}^{nc} x_i m_i\right) - \sum_{i=1}^{nc} x_i(m_i - 1)\ln[g^{HS}(\sigma)] + \frac{P'}{T'\eta}\left(\sum_{i=1}^{nc} x_i m_i\right). \tag{63}$$

The first mixture considered is one of a spherical solvent and a polymer chain of 10 segments, as studied by Paricaud et al. [77]. The second example is a system with a spherical solvent and a polymer chain of 100 segments, and the third mixture is the same solvent with a polymer of 1000 segments.

5.3.1. System C: VLLE in a solvent + polymer system

System C is the first solvent + polymer system considered. The "solvent" has a chain length $m_1 = 1$ and the "polymer" has a chain length of $m_2 = 10$. The T'–x_1 phase diagram for this system at $P' = 0.0037$ is presented in Fig. 7(a). At this pressure the system exhibits VLE, LLE and VLLE. The three-phase line is at $T' = 0.091047$. Below this temperature, there is a small area of liquid–liquid separation (note the large scale of the figure), and an even smaller region of VLE. In the LLE region, the difference in mole fraction between the two phases is $\sim 2 \times 10^{-2}$, and the difference in packing fraction between these phases is $\sim 5 \times 10^{-2}$. The extreme nature of the phase equilibria in this system is further demonstrated by the Gibbs free energy of mixing shown in Fig. 7(b), which exhibits little curvature. Despite the similarity of the coexisting phases, the proposed algorithms do not experience any convergence problems around this liquid–liquid critical point. The details of the calculation at the three-phase line ($T' = 0.91047$ and $P' = 0.0037$) using the Local + Global algorithm are given in Table 5. The procedure of Section 4.5 was employed to refine the composition of the vapour phase.

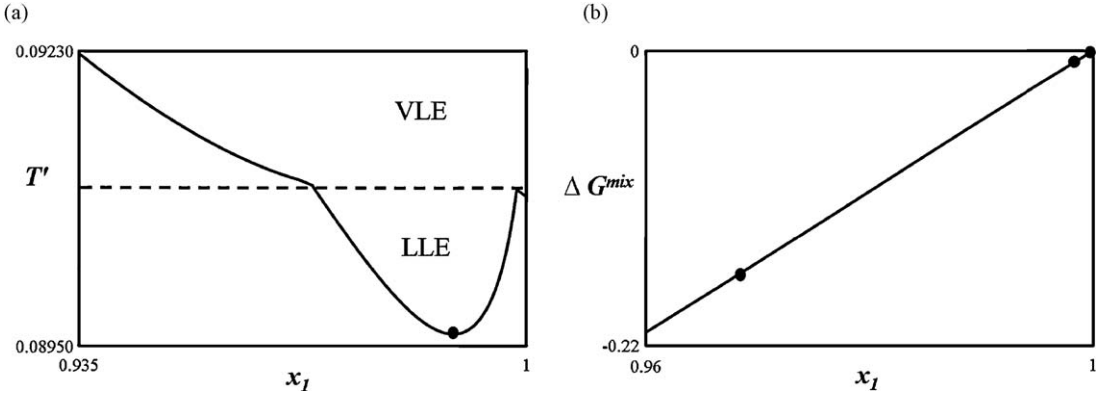

Fig. 7. System C (LLE for an asymmetric binary system with SAFT-HS, solvent $m_1 = 1$, polymer $m_2 = 10$). (a) T'–x_1 diagram showing VLE, LLE and VLLE at $P' = 0.0037$. The continuous curve corresponds to the phase boundary. The liquid–liquid critical point is indicated by a filled circle, and the three-phase temperature of $T' = 0.051865$ by a dashed line. (b) The Gibbs free energy of mixing at $P' = 0.0037$ and $T' = 0.051865$. The filled circles are the stable equilibrium phases present at these conditions. x_1 is the mole fraction of component 1 in the mixture.

Table 5
Stable phases for system C (VLLE for an asymmetric binary system with SAFT-HS, solvent $m_1 = 1$, polymer $m_2 = 10$) at $T' = 0.091047$, $P' = 0.0037$ and $x_1^0 = 0.99$.

	Phase I	Phase II	Phase III
x_1	1.0000 ($x_2 = 4.8 \times 10^{-9}$)	0.9987	0.9687
η	0.0754	0.2073	0.2908

Table 6
Stable phases for system D (VLE for an asymmetric binary system with SAFT-HS, solvent $m_1 = 1$, polymer $m_2 = 100$) at $T' = 0.3$, $P' = 0.01$ and $x_1^0 = 0.99$.

	Phase I	Phase II
x_1	1.0000 ($x_2 = 9.9 \times 10^{-7}$)	0.9530
η	0.0326	0.1526

Table 7
Stable phases for system E (VLE for an asymmetric binary system with SAFT-HS, solvent $m_1 = 1$, polymer $m_2 = 1000$) at $T' = 0.3$, $P' = 0.01$ and $x_1^0 = 0.999$.

	Phase I	Phase II
x_1	1.0000 ($x_2 = 10^{-46}$)	0.9946
η	0.0323	0.1599

5.3.2. Systems D and E: VLE in solvent-polymer systems

We proceed to two test systems with polymers of longer chain lengths, namely $m_2 = 100$ and $m_2 = 1000$. Chains with more than about 100 segments begin to be representative of low molecular weight polymer systems [77]. In terms of size difference, the system with $m_2 = 1000$ would correspond to a real system comprising methane and polyethylene with a molecular mass of around 50,000 g mol^{-1}. The results of point calculations at $P' = 0.01$ and $T' = 0.3$ for both systems are presented in Tables 6 and 7. In Fig. 8(a), the $T' - x_1$ phase diagram is presented for these systems at a reduced pressure of $P' = 0.01$. The behaviour of ΔG^{mix} as a function of the mole fraction of component 1 for both systems is also shown in Fig. 8(b). Both systems exhibit VLE at these conditions, and in both cases there is a very low mole fraction of polymer present in the vapour phase. In system D the vapour phase composition lies within the original bound of 10^{-8}. This is not the case for system E, however, and the procedure outlined in Section 4.5 was employed to improve the solution.

5.4. Computational performance for binary systems

A summary of the computational performance for the calculations with the binary mixtures, with the various algorithmic options, is presented in Table 8. Both iteration numbers and CPU times are reported. Lower CPU times could be achieved with a bespoke implementation. The Local + Global algorithm also requires more overhead than the Global and Global + Constraint versions, because multiple calls are made to the local nonlinear solver. There is a relatively large cost associated with this in GAMS when the subproblems are small, as is the case for the binary systems. The identification of all the phases once the first phase has been found is highly inefficient in the GAMS implementation of all three algorithms as it requires an additional call to the global solver, and the repetition of many calculations. In Table 8, we therefore report the statistics for the identification of the first stable phase only.

As can be seen in Table 8, the first stable phase is identified with certainty in under 6.0 s in all cases, regardless of the type of phase behaviour or the number of phases present. The computational times obtained with the global and local approaches are relatively similar. On problems with few components, it is not expected that the use of a local solver would result in significant savings. Nevertheless, given the additional overhead in this implementation, the Local + Global algorithm can be expected to perform slightly better in a tailored implementation.

The performance of the local version depends greatly on the topology of the $A(\underline{x}, V, T^0)$ surface. The presence of multiple local minima for a given inner problem influences the likelihood of convergence to the global minimum of that inner problem. The initial guesses for the local minimisations are generated randomly and will also affect the outcome. In the examples studied, five local minimisations appeared to be sufficient for a single use of the global routine, apart from the case of system B. When the local minimisation routine is called only twice per inner problem ($N_{local} = 2$), convergence to a local solution of the dual occurred in systems B, D and E. This results in the global routine being called twice, rather than just once as in the calculations where the local solver was called five times ($N_{local} = 5$). The use of the global solver at the final major iteration ensures that the solution found is always globally optimal.

When only global optimisation is employed, the overall iteration count is generally lower, since all iterations are 'useful', i.e., a binding constraint is added to the outer problem. For some of these binary mixtures, the Global version is faster than the Global + Constraint. Including the optimality condition on pressure as a constraint in the global optimisation problem allows the size of the feasible region to be reduced, therefore decreasing the size of the search area. However, the inclusion of additional constraints in the global optimisation problem increases its size.

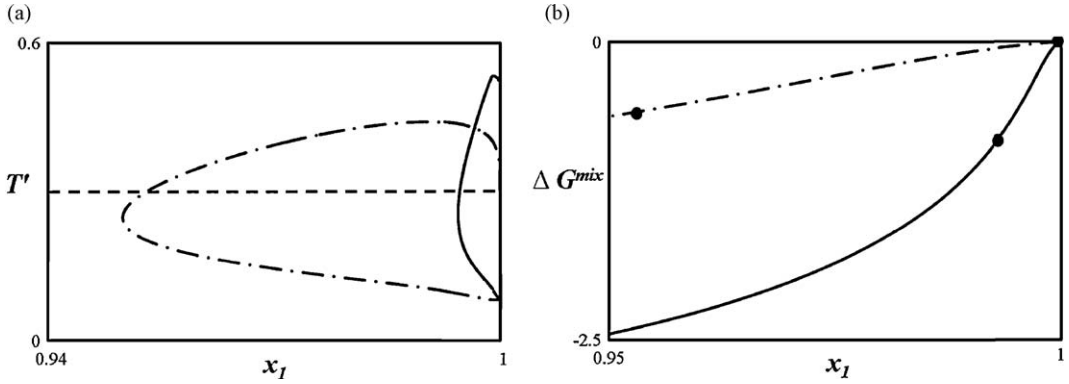

Fig. 8. Systems D and E (VLE for asymmetric binary systems with SAFT-HS, solvent $m_1 = 1$, polymer $m_2 = 100$ and solvent $m_1 = 1$, polymer $m_2 = 1000$, respectively). (a) T'–x_1 plots showing VLE in systems D (dash-dot curve) and E (continuous curve), at $P' = 0.01$. The dashed horizontal line indicates $T' = 0.3$. (b) The Gibbs free energy of mixing in systems D (dash-dot) and E (continuous) at $T' = 0.3$ and $P' = 0.01$. The filled circles are the stable equilibrium phases present at these conditions, marked on each system. x_1 is the mole fraction of component 1 in the mixture.

Table 8
Computational results for point calculations in binary systems (A–E). N_{local} is the number of local solves carried out per inner problem.

System	Method	Major iterations	Local solves	Global opt solves	Total CPU (s)	Global CPU (s)
A	Global	6	–	6	3.3	3.3
A	Global + Constraint	6	–	6	3.1	3.1
A	Local + Global:N_{local} = 2	6	12	1	2.8	0.5
A	Local + Global:N_{local} = 5	6	30	1	4.8	0.4
B	Global	4	–	4	2.0	2.0
B	Global + Constraint	4	–	4	1.6	1.6
B	Local + Global:N_{local} = 2	4	8	2	2.8	1.2
B	Local + Global:N_{local} = 5	4	20	2	4.3	1.2
C	Global	5	–	5	3.4	3.4
C	Global + Constraint	5	–	5	4.1	4.1
C	Local + Global:N_{local} = 2	5	10	1	2.4	0.6
C	Local + Global:N_{local} = 5	5	25	1	4.2	0.6
D	Global	6	–	6	4.3	4.3
D	Global + Constraint	5	–	5	4.4	4.4
D	Local + Global:N_{local} = 2	8	16	2	4.1	1.36
D	Local + Global:N_{local} = 5	6	30	1	4.9	0.7
E	Global	5	–	5	5.8	5.8
E	Global + Constraint	5	–	5	5.8	5.8
E	Local + Global:N_{local} = 2	8	16	2	4.7	1.8
E	Local + Global:N_{local} = 5	7	35	1	6.0	1.0

Table 9
Stable phases for VLE in system F (asymmetric ternary system with SAFT-HS, $m_1 = 1$, $m_2 = 10$, $m_3 = 2$) at $T' = 0.2$, $P' = 0.0037$ and $\underline{x}^0 = (0.4, 0.1, 0.5)^T$.

	Phase I	Phase II
x_1	0.2225	0.4550
x_2	0.3755	0.0148
η	0.1952	0.0340

Table 10
Stable phases for LLE in system F (asymmetric ternary system with SAFT-HS, $m_1 = 1$, $m_2 = 10$, $m_3 = 2$) at $P' = 0.0037$, $T' = 0.091$ and $\underline{x}^0 = (0.98, 0.01, 0.01)^T$.

	Phase I	Phase II
x_1	0.9876	0.9656
x_2	0.0030	0.0229
η	0.2247	0.2800

5.5. Ternary systems modelled with SAFT-HS

We now move onto ternary mixtures modelled with the simplified SAFT-HS EOS. They contain an additional chain component of m_3 spherical segments ($m_3 > 1$), again of diameter σ. This adds an additional variable to the optimisation problems.

5.5.1. System F: VLE and LLE for a ternary mixture

This mixture comprises a spherical solvent $m_1 = 1$ and two chains with $m_2 = 10$ and $m_3 = 2$. The phase diagram for this system at $P' = 0.0037$ and $T' = 0.2$ is shown in Fig. 9(a). At these conditions, the system exhibits VLE over a wide range of composition. We carry out a point calculation at an overall composition of $\underline{x}^0 = (0.4, 0.1, 0.5)^T$. The details of this phase split are reported in Table 9.

We also consider system F at $T' = 0.091$ and $P' = 0.0037$. At these conditions the system exhibits a small region of LLE, close to the solvent apex. The phase diagram for these conditions is shown in Fig. 9(b). Note that the phase diagram is now depicted in weight fraction. In terms of mole fraction the two-phase region would be even smaller. A point calculation is carried out for the global composition $\underline{x}^0 = (0.99, 0.01, 0.01)^T$. The details of the phase split obtained for this composition are shown in Table 10. The performance of the various algorithmic options, for both calculations, is examined in Table 14.

5.5.2. System G: LLLE and LLE for a ternary mixture

We proceed to a yet more asymmetric ternary mixture, of components with $m_1 = 1$, $m_2 = 100$ and $m_3 = 10$. At the conditions of $P' = 0.0037$ and $T' = 0.09$, this system exhibits two regions of LLE, and also a region of LLLE. The phase diagram at these conditions is shown in Fig. 10. Note again that the phase diagram is shown in weight fraction. We conduct point calculations within the two- and three-phase regions. The point within the two-phase region is at a global composition of $\underline{x}^0 = (0.99, 0.005, 0.005)^T$, and the properties of the stable phase split are shown in Table 11. The point within the three-phase region is at a global composition of

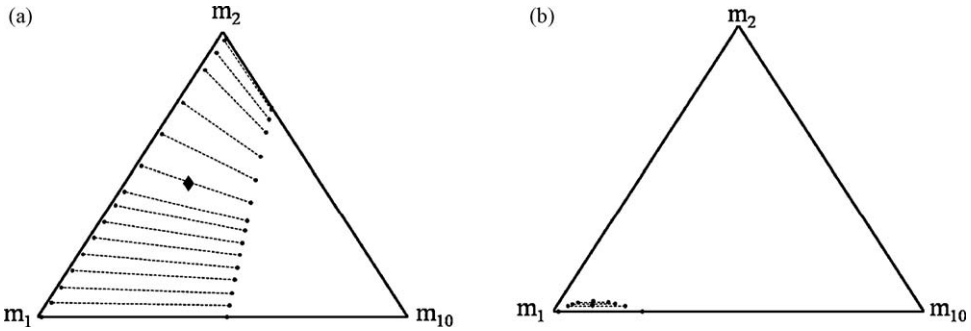

Fig. 9. System F (asymmetric ternary system with SAFT-HS, $m_1 = 1$, $m_2 = 10$, $m_3 = 2$) phase diagrams at $P' = 0.0037$. (a) $T' = 0.2$. Representation in mole fraction. The filled diamond indicates the feed composition used in the point calculation, $\underline{x}^0 = (0.4, 0.1, 0.5)^T$. (b) $T' = 0.091$. Representation in mass fraction. In both (a) and (b), the filled circles are the equilibrium phase compositions and the dotted lines the tie lines.

Table 11
Stable phases for LLE in system G (asymmetric ternary system with SAFT-HS, $m_1 = 1$, $m_2 = 100$, $m_3 = 10$) at $P' = 0.0037$, $T' = 0.09$ and $\underline{x}^0 = (0.99, 0.005, 0.005)^T$.

	Phase I	Phase II
x_1	0.9996	0.9854
x_2	2.2×10^{-16}	0.0074
η	0.2150	0.3408

Table 12
Stable phases for LLLE in system G (asymmetric ternary system with SAFT-HS, $m_1 = 1$, $m_2 = 100$, $m_3 = 10$) at $P' = 0.0037$,$T' = 0.09$ and $\underline{x}^0 = (0.99, 0.0002, 0.0098)^T$.

	Phase I	Phase II	Phase III
x_1	0.9798	0.9953	0.9678
x_2	10^{-5}	10^{-12}	0.0013
η	0.2781	0.2364	0.3116

Table 13
Stable phases for LLLE in system H (asymmetric ternary system with SAFT-HS, $m_1 = 1$, $m_2 = 88.8$, $m_3 = 1000$) at $P' = 0.01$, $T' = 0.0828157$ and $\underline{x}^0 = (0.998701035, 0.001283133, 1.5832 \times 10^{-5})^T$.

	Phase I	Phase II	Phase III
x_1	0.999088	0.998583	0.999301
x_2	0.000912	0.001397	0.000699
η	0.318935	0.327782	0.315933

$\underline{x}^0 = (0.99, 0.0002, 0.0098)^T$, and the properties of the equilibrium phases are shown in Table 12. The concentration of the longest component in the lowest density phase is vanishingly small, and was obtained though the procedure in Section 4.5.

5.5.3. System H: LLLE for a polydisperse mixture

The last ternary mixture for which we show results has been studied in [88]. The model is representative of a polydisperse solvent-polymer mixture. The component chain lengths are $m_1 = 1$, $m_2 = 88.8$ and $m_3 = 1000$. The mixture exhibits LLE at some conditions, and also a very small region of LLLE. To illustrate the complexity of the phase behaviour being studied, we refer to the cloud and shadow curves presented in [88]. These are phase diagrams at a fixed weight ratio of the two polymer molecules, and allow the polymer phase behaviour to be represented over a range of temperatures. Note that this line of fixed weight ratio does not necessarily lie along a tie-line. The phase diagram for $P' = 0.01$ and $T' = 0.0828157$ is shown in Fig. 11. We carry out a point calculation for a temperature and composition within the three-phase region. The Local + Global algorithm accurately identifies the three-phase equilibrium reported in Table 13.

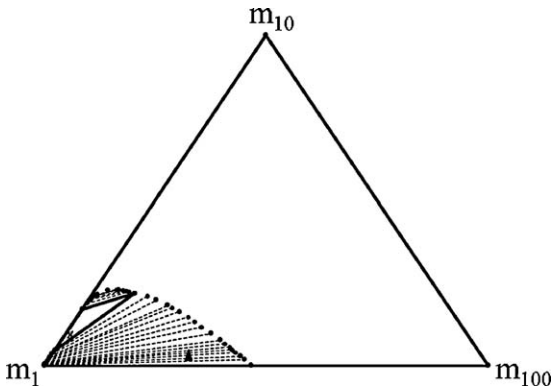

Fig. 10. LLE and LLLE regions for system G (asymmetric ternary system with SAFT-HS, $m_1 = 1$, $m_2 = 100$, $m_3 = 10$) at $P' = 0.0037$ and $T' = 0.09$. The representation is in weight fraction. The filled circles are the equilibrium phase compositions and the dotted lines the tie lines. The three-phase region is outlined by a solid triangle. The point calculation compositions are marked as follows: the cross inside the region of three-phase equilibrium (LLLE) indicates a global composition with mole fraction $\underline{x}^0 = (0.99, 0.0002, 0.0098)^T$. The filled triangle inside the two-phase region indicates a global composition of $\underline{x}^0 = (0.99, 0.005, 0.005)^T$.

5.6. Computational performance for ternary systems

The computational performance of the algorithms for the ternary systems is presented in Table 14. In all cases, the Local + Global algorithm is considerably faster. The difference between the global and local options is more significant here than

Table 14
Computational results for point calculations in ternary systems (F–H). N_{local} is the number of local solves carried out per inner problem.

System	Method	Major iterations	Local solves	Global opt solves	Total CPU (s)	Global CPU (s)
F (VLE)	Global	14	–	14	103.0	103.0
F	Global + Constraint	14	–	14	67.0	67.0
F	Local + Global:$N_{local} = 2$	19	38	5	36.4	28.4
F	Local + Global:$N_{local} = 5$	18	90	2	27.5	12.9
F	Local + Global:$N_{local} = 15$	14	210	1	34.7	5.5
F (LLE)	Global	9	–	9	44.9	44.9
F	Global + Constraint	9	–	9	36.6	36.6
F	Local + Global:$N_{local} = 2$	14	28	3	19.7	13.4
F	Local + Global:$N_{local} = 5$	14	70	2	21.2	9.1
F	Local + Global:$N_{local} = 15$	11	165	1	28.0	4.5
G (LLE)	Global	21	–	21	190.8	190.8
G	Global + Constraint	21	–	21	155.4	155.4
G	Local + Global:$N_{local} = 2$	22	44	4	25.3	16.4
G	Local + Global:$N_{local} = 5$	21	105	1	20.7	3.9
G	Local + Global:$N_{local} = 15$	21	315	1	46.7	4.1
G (LLLE)	Global	15	–	15	72.2	72.2
G	Global + Constraint	13	–	13	65.2	65.2
G	Local + Global:$N_{local} = 2$	14	28	1	11.0	4.6
G	Local + Global:$N_{local} = 5$	17	85	1	18.3	4.5
G	Local + Global:$N_{local} = 15$	16	240	1	37.2	4.6
H (LLLE)	Global	17	–	17	194.4	194.4
H	Global + Constraint	17	–	17	191.4	191.4
H	Local + Global:$N_{local} = 2$	24	48	1	19.1	9.4
H	Local + Global:$N_{local} = 5$	19	95	2	37.0	21.8
H	Local + Global:$N_{local} = 15$	19	285	1	46.6	7.5

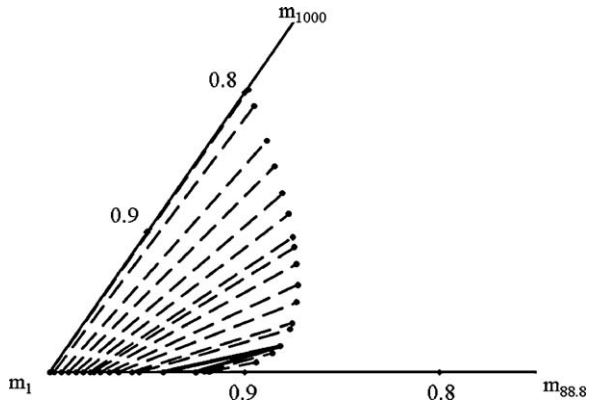

Fig. 11. LLE and LLLE for system H (asymmetric ternary system with SAFT-HS, $m_1 = 1$, $m_2 = 88.8$, $m_3 = 1000$) at $T' = 0.0828157$ and $P' = 0.01$. The representation is in weight fraction. The filled circles indicate the compositions of equilibrium phases and the dashed lines are tie lines. The solid triangle outlines the three-phase (LLLE) region.

with the binary systems, due to the increased size of the problems. The topological influence on the outcome of the local minimisations is also more marked here. The local minimisations on system H converge to a local solution of the dual only once. In contrast, this occurs more frequently with systems F and G. When using $N_{local} = 2$, the longest time is observed for system F (VLE), which requires 36.4 s for global solution of the problem.

The minimum number of iterations required for convergence is also linked to the system topology. Additional factors include the starting value of $\underline{\lambda}$, the feed composition, $\underline{x}^0$, and the required tolerance of convergence in the outer and inner problems. Therefore, for a given tie-simplex (tie-line for two-phase equilibrium, triangle for three-phase equilibrium), the number of iterations required may vary, depending on the position of the global composition within the phase simplex.

6. Conclusions

In this contribution, we have proposed a guaranteed deterministic methodology for solving *P*, *T* fluid phase equilibrium for multi-component mixtures described with general equations of state. The approach is based on the formulation of phase stability as a dual optimisation problem as described by Mitsos and Barton [27]. In order to deal seamlessly with cubic or higher-order equations of state, we reformulate the problem using the Helmholtz free energy, as suggested by Nagarajan et al. [39]. The volume V (or packing fraction) and composition $\underline{x}$ are chosen as the independent variables, and we have shown that the dual problem in the $\underline{x}$ space and the dual problem in the $\underline{x}$–V space have the same solution. The $\underline{x}$–V space possesses several advantageous features. For instance, the Helmholtz free energy is a differentiable function of $\underline{x}$ and V, whereas the Gibbs free energy may not be differentiable everywhere, which can cause problems for gradient-based algorithms. In addition, the computational overheads incurred by repeatedly finding the appropriate volume root at a specified pressure, for each Gibbs free energy evaluation, can be avoided by working in this space. This is particularly useful for higher-than-cubic equations of state and for the development of efficient guaranteed deterministic algorithms.

Having developed the problem formulation, we have presented an algorithm that offers a mathematical guarantee of identifying *all* stable phases in a finite number of iterations within the specified convergence tolerance. The proposed approach is based on the generation of cutting planes at low computational cost, via local optimisation. The combined use of local and global solvers (the Local + Global algorithm with 2 local solves) ensures minimal use of the more computationally expensive global optimisation during the generation of cutting/tangent planes. We have also studied reformulations of the inner problem to speed up its solution, finding that the addition of the first-order optimality condition with respect to volume leads to performance improvements. We have discussed how a spatial branch-and-bound (sBB) global optimisation algorithm may be used to obtain all stable phases present at equilibrium at little additional computational expense once the first stable phase has been found. Finally, we have described a strategy for dealing with components present at very low concentration.

Prototype implementations of the hybrid Local + Global algorithm and two other algorithms based only on global optimisation have been implemented in GAMS with the AVDW and SAFT-HS EOSs. Several challenging calculations have been performed, particularly involving components with a size asymmetry typical of polymer–solvent systems. Phase diagrams have been produced to illustrate the reliability of the method. Thousands of *P*, *T* phase equilibrium problems have been solved reliably to produce these phase diagrams, and no information is carried over from one set of conditions to the next. All systems considered in this paper comprise non-associating components. The presence of associating components leads to an additional term in the SAFT-HS equation, which is usually evaluated with an inner iteration. One could tackle this by adopting an interval-Newton technique as in [30]. Another approach would be to treat the system of equations directly, in the spirit of the volume-composition formulation presented here. This is the direction we are currently pursuing.

The proof-of-concept results obtained in this paper provide one with confidence that the dual formulation is a promising tool for the effective solution of phase equilibrium problems. It is based on the alternating solution of a nonconvex problem and a linear problem, both with up to *nc* variables, where *nc* is the number of components. Furthermore, it is never necessary to guess the number of phases present. We are now planning to investigate the behaviour of the approach with increasing numbers of components and with increasingly sophisticated equations. The approach will be particularly useful in fluid phase equilibrium calculations of anisotropic systems such as liquid crystals, which can also be formulated in the Helmholtz free energy (see for example [89–92]).

Acknowledgements

F.E.P. is grateful to the Engineering and Physical Sciences Research Council (EPSRC) of the UK for a PhD studentship. Additional funding to the Molecular Systems Engineering Group from the EPSRC (grants GR/T17595, GR/N35991, GR/R09497, and EP/E016340), the Joint Research Equipment Initiative (JREI) (GR/M94427), and the Royal Society-Wolfson Foundation refurbishment grant is also acknowledged.

Appendix A. Equivalence of using packing fraction and volume in the inner problem

The mathematical development of the dual formulation is presented throughout the paper in terms of the variable volume, *V*. As mentioned in Section 5, in our GAMS implementation of the inner problem for this algorithm, we use the variable set $\underline{x}$ (composition) and η (packing fraction). η has the desirable property of having clearly defined bounds. In addition, the common SAFT EOSs are often formulated in this variable. In this appendix, we show the equivalence of the lower bounding problem solved in η to that solved in V. We show that the solution to the lower bounding problem lies at the specified pressure, P^0, and that the meaning of $\underline{\lambda}$ remains unchanged. We begin by defining the relationship between

η and V, with η an arbitrary function of $\underline{x}$ and V:

$$V = \frac{f(\underline{x}, T^0)}{\eta}, \tag{A.1}$$

where f is a function that depends on the equation of state used. We will first examine the relationship between the derivatives of the Helmholtz free energy with respect to η and V. We begin by obtaining the derivatives of η with V and x_i:

$$\left(\frac{\partial \eta}{\partial V}\right)_{\underline{x}} = -\frac{f(\underline{x}, T^0)}{V^2} = -\frac{f(\underline{x}, T^0)\eta^2}{f(\underline{x}, T^0)^2} = -\frac{\eta^2}{f(\underline{x}, T^0)}, \tag{A.2}$$

and,

$$\left(\frac{\partial \eta}{\partial x_i}\right)_{x_{j\neq i},V} = \frac{1}{V}\left(\frac{\partial f}{\partial x_i}\right)_{x_{j\neq i}} = \frac{\eta}{f(\underline{x}, T^0)}\left(\frac{\partial f}{\partial x_i}\right)_{x_{j\neq i}}, \quad i = 1, \ldots, nc-1. \tag{A.3}$$

We define a Helmholtz free energy in $\underline{x}$ and η:

$$A'(\underline{x}, \eta; T^0) = A(\underline{x}, V, T^0). \tag{A.4}$$

Then,

$$A'(\underline{x}, \eta; T^0) = \sum_{i=1}^{nc-1}\left(\frac{\partial A'}{\partial x_i}\right)_{x_{j\neq i},\eta} dx_i + \left(\frac{\partial A'}{\partial \eta}\right)_{\underline{x}} d\eta. \tag{A.5}$$

We obtain the derivatives of $A'(\underline{x}, \eta; T^0)$ with respect to composition and volume, for use later in this appendix. We begin with the volume derivatives,

$$\left(\frac{\partial A'}{\partial V}\right)_{\underline{x}} = \left(\frac{\partial A}{\partial V}\right)_{\underline{x}} = \sum_{i=1}^{nc-1}\left(\frac{\partial A'}{\partial x_i}\right)_{x_{j\neq i},\eta}\left(\frac{\mathrm{d}x_i}{\mathrm{d}V}\right)_{\underline{x}} + \left(\frac{\partial A'}{\partial \eta}\right)_{\underline{x}}\left(\frac{\mathrm{d}\eta}{\mathrm{d}V}\right)_{\underline{x}}, \tag{A.6}$$

remarking that

$$\left(\frac{\mathrm{d}x_i}{\mathrm{d}V}\right)_{\underline{x}} = 0, \tag{A.7}$$

Combination of Eqs. (A.2) and (A.6) yields

$$\left(\frac{\partial A'}{\partial V}\right)_{\underline{x}} = -\frac{\eta^2}{f(\underline{x}, T^0)}\left(\frac{\partial A'}{\partial \eta}\right)_{\underline{x}}. \tag{A.8}$$

We may apply a similar treatment to the composition derivatives:

$$\left(\frac{\partial A'}{\partial x_i}\right)_{x_{j\neq i},V} = \left(\frac{\partial A}{\partial x_i}\right)_{x_{j\neq i},V} = \left(\frac{\partial A'}{\partial x_i}\right)_{x_{j\neq i},\eta} + \left(\frac{\partial A'}{\partial \eta}\right)_{\underline{x}}\left(\frac{d\eta}{dx_i}\right)_{x_{j\neq i},V}, \quad i = 1, \ldots, nc-1. \tag{A.9}$$

and combine Eqs. (A.3) and (A.9) to yield

$$\left(\frac{\partial A'}{\partial x_i}\right)_{x_{j\neq i},V} = \left(\frac{\partial A'}{\partial x_i}\right)_{x_{j\neq i},\eta} + \frac{\eta}{f(\underline{x}, T^0)}\left(\frac{\partial f}{\partial x_i}\right)_{x_{j\neq i}}\left(\frac{\partial A'}{\partial \eta}\right)_{\underline{x}}, \quad i = 1, \ldots, nc-1. \tag{A.10}$$

The inner problem, as defined by Eq. (45), is a minimisation in $\underline{x}$ and V. However, we wish to define the inner problem as a minimisation in $\underline{x}$ and η. The Lagrangian, L', in terms of these variables is

$$L'(\underline{x}, \eta, \underline{\lambda}') = A'(\underline{x}, \eta; T^0) + \frac{P^0 f(\underline{x}, T^0)}{\eta} + \sum_{i=1}^{nc-1}\lambda_i'(x_i^0 - x_i) \tag{A.11}$$

The first-order optimality conditions for a minimisation of Eq. (A.11) are

$$\left(\frac{\partial L'}{\partial x_i}\right)_{x_{j\neq i},\eta} = 0 = \left(\frac{\partial A'}{\partial x_i}\right)_{x_{j\neq i},\eta} + \frac{P^0}{\eta}\left(\frac{\partial f}{\partial x_i}\right)_{x_{j\neq i}} - \lambda_i', \tag{A.12}$$

and,

$$\left(\frac{\partial L'}{\partial \eta}\right)_{\underline{x}} = 0 = \left(\frac{\partial A'}{\partial \eta}\right)_{\underline{x}} - \frac{P^0 f(\underline{x}, T^0)}{\eta^2}. \tag{A.13}$$

Combining Eq. (A.8) and Eq. (A.13),

$$-\left(\frac{\partial A}{\partial V}\right)_{\underline{x}}\frac{f(\underline{x}, T^0)}{\eta^2} - \frac{P^0 f(\underline{x}, T^0)}{\eta^2} = 0, \tag{A.14}$$

therefore,

$$\left(\frac{\partial A}{\partial V}\right)_{\underline{x}} + P^0 = 0, \tag{A.15}$$

so that, at the solution of the inner problem in $\underline{x}$ and η,

$$P = P^0. \tag{A.16}$$

Now to prove the equivalence of $\underline{\lambda}$ in the two spaces, we remark from Eq. (A.8) that

$$\left(\frac{\partial A'}{\partial \eta}\right)_{\underline{x}} = P\frac{f(\underline{x}, T^0)}{\eta^2}, \tag{A.17}$$

hence at the solution of the inner problem the following expression holds:

$$\left(\frac{\partial A'}{\partial \eta}\right)_{\underline{x}} = P^0\frac{f(\underline{x}, T^0)}{\eta^2}. \tag{A.18}$$

Combining the Karush–Kuhn–Tucker (KKT) conditions Eq. (A.12) with Eq. (A.10) produces,

$$\left(\frac{\partial A'}{\partial x_i}\right)_{x_{j\neq i},V} - \frac{\eta}{f(\underline{x}, T^0)}\left(\frac{\partial f}{\partial x_i}\right)_{x_{j\neq i}}\left(\frac{\partial A'}{\partial \eta}\right)_{\underline{x}} + \frac{P^0}{\eta}\left(\frac{\partial f}{\partial x_i}\right)_{x_{j\neq i}} - \lambda_i' = 0, \quad \text{for } i = 1, \ldots, nc-1. \tag{A.19}$$

Finally, using Eq. (A.18), at the solution,

$$\left(\frac{\partial A'}{\partial x_i}\right)_{x_{j\neq i},V} - \lambda_i' = 0 \tag{A.20}$$

i.e., the Lagrange multipliers in the $(\underline{x}, \eta)$ space and the $(\underline{x}, V)$ space are equivalent:

$$\lambda_i' = \lambda_i, \quad \text{for } i = 1, \ldots, nc-1 \tag{A.21}$$

References

[1] C.Y. Gau, J.F. Brennecke, M.A. Stadtherr, Reliable nonlinear parameter estimation in VLE modeling, Fluid Phase Equilibria 168 (2000) 1.
[2] A. Giovanoglou, A. Galindo, G. Jackson, C.S. Adjiman, Fluid phase stability and equilibrium calculations in binary mixtures. Part I. Theoretical development for non-azeotropic mixtures, Fluid Phase Equilibria 275 (2009) 79.
[3] A. Giovanoglou, C.S. Adjiman, G. Jackson, A. Galindo, Fluid phase stability and equilibrium calculations in binary mixtures. Part II. Application to single-point calculations and the construction of phase diagrams, Fluid Phase Equilibria 275 (2009) 95.
[4] W.B. White, S.M. Johnson, G.B. Dantzig, Chemical equilibrium in complex mixtures, The Journal of Chemical Physics 28 (1958) 751.
[5] J. Castillo, I.E. Grossmann, Computation of phase and chemical equilibria, Computers and Chemical Engineering 5 (1981) 99.
[6] M.L. Michelsen, The isothermal flash problem. Part I. Stability, Fluid Phase Equilibria 9 (1982) 1.
[7] M.L. Michelsen, The isothermal flash problem. Part II. Phase-split calculation, Fluid Phase Equilibria 9 (1982) 21.

[8] M.L. Michelsen, J.M. Mollerup, Thermodynamic Models: Fundamentals and Computational Aspects, second edition, Tie-line Publications, Holte, Denmark, 2007.
[9] R. Gautam, W.D. Seider, Computation of phase and chemical equilibrium. Part I. Local and constrained minima in Gibbs free energy, AIChE Journal 25 (1979) 991.
[10] R. Gautam, W.D. Seider, Computation of phase and chemical equilibrium. Part II. Phase splitting, AIChE Journal 25 (1979) 999.
[11] A.C. Sun, W.D. Seider, Homotopy-continuation method for stability analysis in the global minimization of the Gibbs free energy, Fluid Phase Equilibria 103 (1995) 213.
[12] M.E. Soares, A.G. Medina, C. McDermott, N. Ashton, Three-phase flash calculations using free energy minimisation, Chemical Engineering Science 37 (1982) 521.
[13] L.T. Biegler, L.G. Bullard, Iterated linear programming strategies for non-smooth simulation: A penalty based method for vapor liquid equilibrium applications, Computers and Chemical Engineering 17 (1993) 95.
[14] A. Lucia, L. Padmanabhan, S. Venkataraman, Multiphase equilibrium flash calculations, Computers and Chemical Engineering 24 (2000) 2557.
[15] A. Lucia, P.A. DiMaggio, M.L. Bellows, L.M. Octavio, The phase behavior of *n*-alkane systems, Computers and Chemical Engineering 29 (2005) 2363.
[16] A. Lucia, X. Guo, P.J. Richey, R. Derebail, Simple process equations, fixed-point methods, and chaos, AIChE Journal 36 (1990) 641.
[17] K.A. Green, S. Zhou, K.D. Luks, The fractal response of robust solution techniques to the stationary point problem, Fluid Phase Equilibria 84 (1993) 49.
[18] J.Z. Hua, J.F. Brennecke, M.A. Stadtherr, Enhanced interval analysis for phase stability: Cubic equation of state models, Industrial Engineering and Chemistry Research 37 (1998) 1519.
[19] M.L. Michelsen, State function based flash specifications, Fluid Phase Equilibria 158–160 (1999) 617.
[20] D.V. Nichita, S. Gomez, E. Luna, Multiphase equilibria calculation by direct minimization of Gibbs free energy with a global optimization method, Computers and Chemical Engineering 26 (2002) 1703.
[21] C.M. McDonald, C.A. Floudas, Decomposition based and branch and bound global optimization approaches for the phase equilibrium problem, Journal of Global Optimization 5 (1994) 205.
[22] C.M. McDonald, C.A. Floudas, Global optimization for the phase stability problem, AIChE Journal 41 (1995) 1798.
[23] C.M. McDonald, C.A. Floudas, Global optimization and analysis for the Gibbs free energy function using the UNIFAC, Wilson and ASOG equations, Industrial and Engineering Chemistry Research 34 (1995) 1674.
[24] C.M. McDonald, C.A. Floudas, GLOPEQ: A new computational tool for the phase and chemical equilibrium problem, Computers and Chemical Engineering 21 (1997) 1.
[25] S.T. Harding, C.A. Floudas, Phase stability with cubic equations of state: global optimization approach, AIChE Journal 46 (2000) 1422.
[26] S.T. Harding, C.A. Floudas, Locating all heterogeneous and reactive azeotropes in multicomponent mixtures, Industrial and Engineering Chemistry Research 39 (2000) 1576.
[27] A. Mitsos, P.I. Barton, A dual extremum principle in thermodynamics, AIChE Journal 53 (2007) 2131.
[28] J.Z. Hua, J.F. Brennecke, M.A. Stadtherr, Reliable prediction of phase stability using an interval Newton method, Fluid Phase Equilibria 116 (1996) 52.
[29] K. McKinnon, M. Mongeau, A generic global optimization algorithm for the chemical and phase equilibrium problem, Journal of Global Optimization 12 (1998) 325.
[30] G. Xu, J.F. Brennecke, M.A. Stadtherr, Reliable computation of phase stability and equilibrium from the SAFT equation of state, Industrial and Engineering Chemistry Research 41 (2002) 938.
[31] A.T. Souza, L. Cardozo-Filho, F. Wolff, R. Guirardello, Application of interval analysis for Gibbs and Helmholtz free energy global minimization in phase stability analysis, Brazilian Journal of Chemical Engineering 23 (2006) 117.
[32] G.P. Rangaiah, Evaluation of genetic algorithms and simulated annealing for phase equilibrium and stability problems, Fluid Phase Equilibria 187 (2001) 83.
[33] M. Srinivas, G.P. Rangaiah, A study of differential evolution and tabu search for benchmark, phase equilibrium and phase stability problems, Computers and Chemical Engineering 31 (2007) 760.
[34] D.V. Nichita, S. Gomez, E. Luna, Phase stability analysis with cubic equations of state by using a global optimization method, Fluid Phase Equilibria 194–197 (2002) 411.
[35] W.A. Wakeham, R.P. Stateva, Numerical solution of the isothermal, isobaric phase equilibrium problem, Reviews in Chemical Engineering 20 (2004) 1.
[36] H. Segura, I. Polishuk, J. Wisniak, Phase stability analysis in binary systems, Physics and Chemistry of Liquids 38 (2000) 277.
[37] W.G. Chapman, K.E. Gubbins, G. Jackson, M. Radosz, SAFT: equation of state solution model for associating fluids, Fluid Phase Equilibria 52 (1989) 31.
[38] W.G. Chapman, K.E. Gubbins, G. Jackson, M. Radosz, New reference equation of state for associating liquids, Industrial and Engineering Chemistry Research 29 (1990) 1709.
[39] N.R. Nagarajan, A.S. Cullick, A. Griewank, New strategy for phase equilibrium and critical point calculations by thermodynamic energy analysis. Part 1. Stability analysis and flash, Fluid Phase Equilibria 62 (1991) 191.
[40] N.R. Nagarajan, A.S. Cullick, A. Griewank, New strategy for phase equilibrium and critical point calculations by thermodynamic energy analysis. Part II. Critical point calculations, Fluid Phase Equilibria 62 (1991) 211.
[41] D.V. Nichita, C. de Los Angeles Duran Valencia, S. Gomez, Volume-based thermodynamics global phase stability analysis, Chemical Engineering Communications 193 (2006) 1194.
[42] A. Mitsos, G.M. Bollas, P.I. Barton, Bilevel optimization formulation for parameter estimation in liquid–liquid phase equilibrium problems, Chemical Engineering Science 64 (2009) 548.
[43] G.M. Bollas, P.I. Barton, A. Mitsos, Bilevel optimization formulation for parameter estimation in vapor–liquid (-liquid) phase equilibrium problems, Chemical Engineering Science 64 (2009) 1768.
[44] L.E. Baker, A.C. Pierce, K.D. Luks, Gibbs energy analysis of phase equilibria, SPE Journal 22 (1982) 731.
[45] J.A. Beattie, Thermodynamics and Physics of Matter, Section C: Thermodynamic Properties of Real Gases and Mixtures of Real Gases, Oxford University Press, 1955.
[46] M.S. Bazaraa, H.D. Sherali, C.M. Shetty, Nonlinear Programming; Theory and Algorithms, second edition, John Wiley and Sons, New York, 1993.
[47] H. Triebel, Analysis and Mathematical Physics, Kluwer Academic Publishers, Dordrecht, 1986.
[48] M. Modell, R.C. Reid, Thermodynamics and its Applications, Prentice Hall, 1983.
[49] C.M. McDonald, C.A. Floudas, Global optimization for the phase and chemical equilibrium problem: application to the NRTL equation, Computers and Chemical Engineering 19 (1995) 1111.
[50] C.A. Floudas, Deterministic Global Optimization; Theory, Methods and Applications, Kluwer Academic Publishers, Dordrecht, 2000.
[51] N.V. Sahinidis, BARON: a general purpose global optimization software package, Journal of Global Optimization 8 (1996) 201.
[52] N.V. Sahinidis, M. Tawarmalani, BARON with GAMS User Guide, www.gams.com/solvers, 2009.
[53] I.P. Androulakis, C.D. Maranas, C.A. Floudas, αBB: a global optimization method for general constrained nonconvex problems, Journal of Global Optimization 7 (1995) 337.
[54] C.S. Adjiman, S. Dallwig, C.A. Floudas, A. Neumaier, A global optimization method, αBB, for general twice-differentiable constrained NLPs. I. Theoretical advances, Computers and Chemical Engineering 22 (1998) 1137.
[55] C.D. Maranas, C.A. Floudas, Finding all solutions of nonlinearly constrained systems of equations, Journal of Global Optimization 7 (1995) 143.
[56] C.A. Schnepper, M.A. Stadtherr, Robust process simulation using interval methods, Computers and Chemical Engineering 20 (1996) 187.
[57] J.W. Blankenship, F.E. Falk, Infinitely constrained optimization problems, Journal of Optimization Theory and Applications 19 (1976) 261.
[58] S.A. Gustafson, A three-phase algorithm for semi-infinite programs, in: A.V. Fiacco, K.O. Kortanek (Eds.), Semi-infinite Programming and Applications, Springer, Berlin, 1983, p. 138.
[59] R. Hettich, K.O. Kortanek, Semi-infinite programming: theory, methods, and applications, SIAM Review 35 (1993) 380.
[60] C.A. Floudas, C.E. Gounaris, A review of recent advances in global optimization, Journal of Global Optimization 45 (2009) 3.
[61] Z.H. Gümüş, C.A. Floudas, Global optimization of nonlinear bilevel programming problems, Journal of Global Optimization 20 (2001) 1.
[62] A. Mitsos, P. Lemonidis, P.I. Barton, Global solution of bilevel programs with a nonconvex inner program, Journal of Global Optimization 42 (2008) 475.
[63] A. Tsoukalas, B. Rustem, E.N. Pistikopoulos, A global optimization algorithm for generalized semi-infinite, continuous minimax with coupled constraints and bi-level problems, Journal of Global Optimization 44 (2009) 235.
[64] A. Tsoukalas, W. Wiesemann, B. Rustem, Global optimisation of pessimistic bi-level problems, in: Lectures on Global Optimization, vol. 55 of Fields Inst. Commun., Amer. Math. Soc., Providence, RI, 2009, p. 215.
[65] H.D. Sherali, H. Wang, Global optimization of nonconvex factorable programming problems, Mathematical Programming 89 (2001) 459.
[66] H.D. Sherali, A. Alameddine, A new reformulation-linearization technique for bilinear programming problems, Journal of Global Optimization 2 (1992) 379.
[67] L. Liberti, Reduction constraints for the global optimization of NLPS, International Transactions in Operational Research 11 (2004) 33.
[68] L. Liberti, C.C. Pantelides, An exact reformulation algorithm for large nonconvex NLPs involving bilinear terms, Journal of Global Optimization 36 (2006) 161.
[69] C.S. Adjiman, I.P. Androulakis, C.A. Floudas, A global optimization method, αBB, for general twice-differentiable constrained NLPs. II. Implementation and computational results, Computers and Chemical Engineering 22 (1998) 1159.
[70] R. Horst, H. Tuy, Global Optimization: Deterministic Approaches, third edition, Springer-Verlag, Berlin, 1996.
[71] B.J. Alder, C.E. Hecht, Studies in molecular dynamics. VII. Hard-sphere distribution functions and an augmented van der Waals theory, Journal of Chemical Physics 50 (1969) 2032.
[72] K.N. Marsh, M.L. McGlashan, C. Warr, Thermodynamic excess functions of mixtures of simple molecules according to several equations of state, Transactions of the Faraday Society 66 (1970) 2453.
[73] N.F. Carnahan, K.E. Starling, Intermolecular repulsions and the equation of state for fluids, AIChE Journal 18 (1972) 1184.
[74] G. Jackson, J.S. Rowlinson, C.A. Leng, Phase equilibria in model mixtures of spherical molecules of different sizes, Journal of the Chemical Society, Faraday Transactions 1 82 (1986) 3461.
[75] A. Galindo, P.J. Whitehead, G. Jackson, A.N. Burgess, Predicting the high-pressure phase equilibria of water + n-alkanes using a simplified SAFT theory with transferable intermolecular interaction parameters, Journal of Physical Chemistry 100 (1996) 6781.

[76] P.H. van Konynenburg, R.L. Scott, Critical lines and phase equilibria in binary van der Waals mixtures, Philosophical Transactions of the Royal Society of London A 298 (1980) 495.
[77] P. Paricaud, A. Galindo, G. Jackson, Understanding liquid–liquid immiscibility and LCST behaviour in polymer solutions with a Wertheim TPT1 description, Molecular Physics 101 (2003) 2575.
[78] General Algebraic Modelling System (GAMS), www.gams.com, 2009.
[79] B.A. Murtagh, M.A. Saunders, P.E. Gill, Minos with GAMS User Guide, www.gams.com/solvers, 2009.
[80] GAMS Development Corporation, CPLEX 12 with GAMS User Guide, www.gams.com/solvers, 2007.
[81] J.S. Rowlinson, F.L. Swinton, Liquids and Liquid Mixtures, Butterworth, London, 1982.
[82] A. Galindo, P.J. Whitehead, G. Jackson, A.N. Burgess, Predicting the phase equilibria of mixtures of hydrogen fluoride with water, difluoromethane (HFC-32), and 1,1,1,2-tetrafluoroethane (HFC-134a) using a simplified SAFT approach, Journal of Physical Chemistry B 101 (1997) 2082.
[83] W.G. Chapman, G. Jackson, K.E. Gubbins, Phase equilibria of associating fluids: chain molecules with multiple bonding sites, Molecular Physics 65 (1988) 1057.
[84] D.G. Green, G. Jackson, Theory of phase equilibria and closed-loop liquid–liquid immiscibility for model aqueous solutions of associating chain molecules: water + alkanol mixtures, Journal of Chemical Physics 97 (1992) 8672.
[85] D.G. Green, G. Jackson, Theory of phase equilibria for model aqueous solutions of chain molecules: water + alkane mixtures, Journal of the Chemical Society, Faraday Transactions 88 (1992) 1395.
[86] G. Jackson, Theory of closed-loop liquid–liquid immiscibility in mixtures of molecules with directional attractive forces, Molecular Physics 72 (1991) 1365.
[87] N.F. Carnahan, K.E. Starling, Equation of state for nonattracting rigid spheres, Journal of Chemical Physics 51 (1969) 635.
[88] P. Paricaud, A. Galindo, G. Jackson, Examining the effect of chain length polydispersity on the phase behavior of polymer solutions with the statistical associating fluid theory (Wertheim TPT1) using discrete and continuous distributions, Journal of Chemical Physics 127 (2007) 154906.
[89] D.C. Williamson, G. Jackson, Liquid crystalline phase behavior in systems of hard-sphere chains, Journal of Chemical Physics 108 (1998) 10294.
[90] M. Franco-Melgar, A.J. Haslam, G. Jackson, A generalisation of the Onsager trial-function approach: describing nematic liquid crystals with an algebraic equation of state, Molecular Physics 106 (2008) 649.
[91] M. Franco-Melgar, A.J. Haslam, G. Jackson, Advances in generalised van der Waals approaches for the isotropic-nematic fluid phase equilibria of thermotropic liquid crystals—an algebraic equation of state for attractive anisotropic particles with the Onsager trial function, Molecular Physics 107 (2009) 2329.
[92] A. Malijevský, G. Jackson, S. Varga, Many-fluid Onsager density functional theories for orientational ordering in mixtures of anisotropic hard-body fluids, Journal of Chemical Physics 129 (2008) 144504.